2012

Elucidating the role of bone morphogenetic proteins and b-lymphocyte maturation protein 1 during primordial germ cell specification

Laughing Bear Torrez Dulgeroff

ELUCIDATING THE ROLE OF BONE MORPHOGENETIC PROTEINS AND B-LYMPHOCYTE MATURATION PROTEIN 1 DURING PRIMORDIAL GERM CELL SPECIFICATION

A Thesis

Presented to the

Faculty of

California State University,

San Bernardino

In Partial Fulfillment

of the Requirements for the Degree

Master of Science

in

Biology

---

by

Laughing Bear Torrez Dulgeroff

June 2012

ELUCIDATING THE ROLE OF BONE MORPHOGENETIC PROTEINS AND B-LYMPHOCYTE MATURATION PROTEIN 1 DURING PRIMORDIAL GERM CELL SPECIFICATION

A Thesis

Presented to the

Faculty of

California State University,

San Bernardino

---

by

Laughing Bear Torrez Dulgeroff

June 2012

Approved by:

[redacted]

Dr. Nicole Bourmias-Vardiabasis, Chair, Biology

06/08/2012

Date

[redacted]

Dr. Duncan Liew

[redacted]

Dr. Jeffrey Thompson

ABSTRACT

Human embryonic stem cells (hESC) and induced pluripotent stem cells (iPSC) provide a model for studying paradigms of early human development. Techniques that quantify transcriptional activity, protein expression and chromatin modification as hESC and hiPSC differentiate can be used to decipher the changes that are responsible for specification and development of cellular lineages. This thesis presents an optimized protocol to induce and isolate primordial germ cells (PGC) from hESC and hiPSC. Time-course experiments revealed that bone morphogenetic protein (BMP) signals play an essential role in inducing BLIMP1-expressing PGC from both hESC and hiPSC. Magnetic activated cell sorting for cell surface marker CXCR-4 allowed the isolation of cells with PGC gene expression profiles. PCR and genetic manipulation was used to determine the specific variance of BLIMP1, a transcriptional repressor, which initiates PGC identity. We identified BLIMP1a as the variance responsible for the activation of a restricted PGC fate and repression of the somatic cell program. The expression of BLIMP1 was shown to directly target pluripotency gene OCT4. Furthermore, a novel function for BLIMP1 during epigenetic reprogramming of the germline is presented. Expression of BLIMP1 was significantly correlated with histone modification, specifically the occurrence of histone 3 lysine 27 trimethylation.

ACKNOWLEDGEMENTS

Funding for this research was generously provided by the California Institute of Regenerative Medicine Brides Stem Cell Scholar Program. I would like to acknowledge the efforts of Dr. Nicole Bournias and Dr. Jeffrey Thompson for bringing the CIRM Bridges program to CSUSB. With additional help from Dave Coffey, intense course work was designed to prepare CIRM scholars for assignment in stem cell culture laboratories. Admission to the CIRM Bridges program, contingent upon recommendation from Dr. Mike Chao, Dr Antony Metcalf and Dr. James Ferrari, made a lasting impact on who I was as a graduate student and the scientist I will become. Thank you for your continuous support and guidance.

Most of all I would like to recognize my mentor Dr. Duncan Liew. I was fortunate to be placed under your supervision and I am a better scientist for it. You continually pushed me to be precise in my technique, rigorous in analysis and professional in presentation and it has helped me achieve goals that I never thought possible.

Last, I would like to thank my family. My mother and father who have continually supported my education, and have always encouraged me do to what makes me happy. My brother, who always was and always will be there for me. And last, but never least, James thank you for your love and patience.

TABLE CONTENTS

LIST OF TABLES

LIST OF FIGURES

CHAPTER ONE

INTRODUCTION

Pluripotent Stem Cell Models

A pivotal advance concerning human development and disease has been the discovery of human pluripotent stem cells. Pluripotent describes any population of cells which undergo mitotic division to form self-renewing daughter cells, which maintain the capacity to differentiate to mature cells types of all three germ layers (Weissman et al., 2001). Pluripotent cells can be compared to other stem cells types; totipotent cells can form an entire organism including extraembryonic tissues, multipotent cells form several cell types but are more limited in lineage differentiation, and unipotent cells only differentiate into a single cell type.

The most common source of human pluripotent cells are from the inner cell mass (ICM) of a five-to-eight day human blastocyst. Human embryonic stem cells (hESC) were first isolated from donated *in vitro* fertilized (IVF) eggs. The ICM of preimplantation stage embryos were isolated and initially grown in culture with the support of mouse fibroblast feeder layers (Thompson et al., 1998a). Potency of the ICM-harvested cells was established by comparing morphology, telomerase activity, pluripotency-associated gene expression, and differentiation capacity for derivatives from all three germ layers; determined in previous non-

human primate embryonic stem cell foundational studies (Thompson et al.,1995 ; Thompson et al., 1998b).

Given ethical concerns regarding the destruction of preimplantation stage human embryos adult derived populations of pluripotent stem cells were sought out. The goal was to voluntarily isolate adult tissues and then genetically manipulated them in order to re-establish the pluripotency. Accordingly, these cells would not only be harvested from an ethical source but could also serve as therapeutically autologous cells for transplantation. By over-expressing pluripotency-associated genes, highly expressed in hESC, adult cells were demonstrated to be induced to regress to a pluripotent state. Genetically manipulated adult derived pluripotent cells are known as human induced pluripotent stem cells (hiPSC). The most prominent protocol for deriving hiPSC involves retroviral reprogramming of adult fibroblast cells to promote the expression of ESC specific transcription factors: OCT4, Sox2, KLF4 and c-MYC (Takahashi et al., 2007). These specific transcription factors were selected from 24 candidate genes that regulate the ESC identity and were evaluated for their ability to reprogram somatic cells (Takahashi et al., 2006). Given the hiPSC reprogramming protocol, a readily available and ethically acceptable source (i.e. not an embryonic cell source) of pluripotent cells was defined.

The derivation hESC and hiPSC has opened up an entirely novel field in which human development and disease, previously restricted to animal modeling, can be readily manipulated.

In the past modeling of molecular and cellular level processes have been restricted to animal model systems. While animal models have contributed to our understanding of important developmental processes that relate to human development there are several drawbacks to this approach. Animal models can only be used to accurately study processes that are evolutionarily conserved and even then subtle but significant differences exist. For example in the field of stem cell biology several major distinctions exist between two commonly compared species, human and mouse. Human ICM are harvested from the preimplantation blastocyst, a characteristic that enables ethical harvesting. Comparative analysis of hESC to both preimplantation mouse embryonic stem cells (mESC) and mouse postimplantation epiblast-derived stem cells (mEpiSC) revealed that EpiSC share gene expression patterns and respond to signals similarly to hESC (Tesar et al., 2007). Also, hESC and mESC and mEpiSC share expression of several cell surface markers including stage specific embryonic antigens three (SSEA3) and four (SSEA4), cell surface expression of SSEA1 is associated with differentiation in hESC compared to pluripotency in mESC and EpiSC (Henderson et al., 2002). However, mESC and mEpiSC are both distinct from hESC in the expression of cell surface marker stage specific embryonic antigen 1 (SSEA1). Furthermore, the two species differ regarding molecular mechanisms of self-renewal. Maintenance of self-renewal in mESC relies on the presence of leukemia inhibitory factor (LIF) which binds the leukemia inhibitory factor receptor (LIFR). Consequently, activation of LIFR by LIF initiates a molecular cascade

involving signal transducer and activator of transcription 3 (STAT3). On the other hand, it has been demonstrated that STAT3 signaling pathways are not activated in human embryonic stem cells (hESC) to regulate self-renewal and therefore do not require LIF in culture medium (Dahéron et al., 2004). The aforementioned paradigms highlight the importance of examining development and disease in human models, in addition to foundational studies in other animal model systems.

Once the pluripotent cells, hESC or hiPSC, are derived, they possess unlimited potential for researching any cell type of the human anatomy including significant precursors of ectoderm, mesoderm, endoderm and germline lineages (Figure 1). Cell culture of pluripotent cells coupled with molecular biology techniques have been used extensively to study previously impenetrable lineage development in order to elucidate the underlying molecular mechanisms of differentiation from derivatives of all three germ layers: endoderm, mesoderm and ectoderm (Wang et al., 2011; Xu et al., 2012; Sasaki et al., 2010).

Furthermore, hESC and hiPSC have important implications in disease modeling. Potentially, hiPSC specifically reprogrammed from adult cells collected from the tissue of an individual with a diseased phenotype could be readily used to model and interrogate the development of the disease *in vitro*. The practice

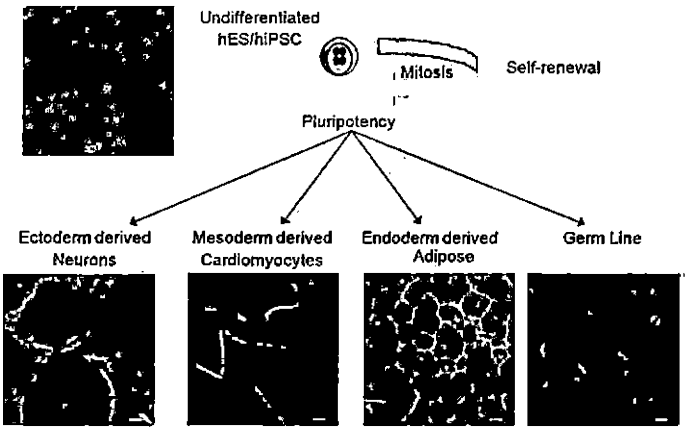

Figure 1. Overview of Pluripotency. Pluripotent cells must have a low cytoplasm to nucleus ratio, with prominent nuclei. The cells must be capable of mitotic self-renewal and the ability to differentiate into all three germ layers, as well as germ cells. Scale bars are 50μm. (Aw TJ, Haas SJ, Liew D, Krum H. 2005. Meta-analysis of Cyclooxygenase-2 Inhibitors and Their Effects on Blood Pressure. Arch Intern Med 165:490–496.)

of collecting tissues from diseased individuals and reprogramming those cells into hiPSC has become well known as the "disease in a dish" model. Diseased hiPSC can be manipulated to delineate underlying mechanisms of the disease and its development. Cardiac diseases, related to several DNA variations, have been described, but the effects of these variations are not known (Kathiresan et al., 2009). Thus hiPSC from patients with cardiac disease can be used to determine the underlying mechanism of the DNA variations and their progression to the diseased phenotype. Similarly, patient specific hiPSC have also been proposed as a source of cells to clinically combat degenerative diseases. For example, hiPSC used to generate dopaminergic neurons have the potential to

cure idiopathic Parkinson's disease (Soldner et al., 2009). The disease in a dish model has also become widespread in laboratories focusing on drug discovery, and is being used in parallel with animal-based drug testing. For example, BGP-15, a pharmacological inducer of heat shock protein 72 was recently used by disease in a dish modeling to reduce the progression of Duchenne muscular dystrophy (Gehrig, 2012).

Primordial Germ Cell Differentiation

This work addresses a highly unique and understudied lineage of consequence, the germline. Germ cells arise from a niche located in the proximal posterior epiblast, which enables the cells to avoid signaling factors from the primitive streak (Wylie, 2000). Signaling from the surrounding somatic niches leads to the expression of the transcriptional regulator of the germline, B-lymphocyte maturation protein 1 (BLIMP1) (Ohinata et al., 2005). BLIMP1 expression initiates specification of primordial germ cells (PGC). Following the onset of specification, the cells undergo mitosis and begin migration across the genital ridges. The cells will continue to replicate as well as upregulate germ cell transcripts (Kurimoto et al., 2008). Ultimately, PGC colonize the gonads and mature into haploid gametes (Tam et al., 1981).

Germ cells are distinguishable from all other somatic lineages and undergo several unique processes. Development of somatic cell types requires switching from a pluripotent identity to a differentiated state, as indicated by

coincident differentiation following OCT4 knockdown (Hay et al., 2004). As germ cells differentiate, their survival is dependent upon the maintenance of OCT4 (Kehler et al., 2004), which is unsurprising given the characteristic pluripotent designation of the germline. The maintenance of pluripotency as germ cells differentiate is highly unique. Given the unique model of pluripotency it has been proposed that exploring the development and formation of the germline can help explain how adult stem cells niches maintain self-renewal and a multipotent differentiation potential (Lanza, 2009). In fact, multipotent adult stem cell niches have been identified in several tissues, including epidermal, follicular, intestinal, neuronal, and hematopoietic niches (Fuchs and Segre, 2000).

Germline modeling also provides the opportunity to study reprogramming of the epigenome. Epigenetics involves the regulation of gene transcription without affecting the deoxyribose nucleic acid (DNA) sequence itself. The heritability of the correct epigenetic code from parent to offspring is pivotal and requires thorough examination. Alteration of the normal epigenome can result in major degenerative diseases, like cancer, Angelman's syndrome, Beckwith–Wiedemann syndrome and Prader–Willi syndrome. Epigenetic therapies aim to inhibit epigenetic modifiers in order to regulate chromatin accessibility. While the epigenetic enzymes targeted in these therapies are determined based on germline epigenetic reprogramming, there are few studies that focus on molecular mechanisms that initiate reprogramming in the germ cells. (Egger et al., 2004).

Research of germline development will also contribute to therapeutic efforts to combat infertility. Every year 12 couples out of 10,000 struggle with infertility (Hull et al., 1985). Depicting the stage specific molecular interactions involved in the differentiation of human germ cells provides a tool for interrogating and ameliorating qualitative and quantitative causes of infertility. Ultimate goals of describing germline differentiation can also be used to optimize protocols for deriving germ cells *in vitro* from patient specific hiPSC.

Research Aims

Currently there is a minimal amount of research on the human germline, and moreover on the specification of human primordial germ cells (PCG). The germline is especially difficult to study given the ethical constraints of harvesting embryonic germ cells from human embryos, as well as the prohibition of genetic manipulation of human embryos, preventing examination of key developmental genes in human. Using hESC and hiPSC, the molecular mechanisms of germline specification were examined using murine model paradigms. This thesis describes the following aims concerning germline specification:

1) Efficient induction and isolation of PGC

2) Determining the specific transcriptional regulator of the germline

3) Observing early epigenetic changes of the germline

Efficient Induction and Isolation of Primordial Germ Cells

Relatively little is known about specific pathways that control PGC commitment in early human embryonic development and the hESC model, but it is becoming evident that specific pathways may differ substantially between mouse and human development. One example of non-evolutionarily conserved molecular mechanisms across mice and humans involves BMP4. BMP4 has been extensively used to maintain the mouse stem cell phenotype. Conversely, blocking BMP4 signaling along with addition of bFGF to hESC cultures has been demonstrated to suppress differentiation and maintain pluripotency in hESC (Xu et al., 2005). Furthermore, BMP signaling in human embryos has been associated with the bone differentiation and hematopoiesis (Chadwick et al., 2003; Cheng et al., 2003). Additionally, negative regulation of BMP signaling has been used to restrict differentiation to specific lineages. The addition of Noggin to differentiating hECS antagonizes BMP signaling and is used to induce the differentiation of neuronal precursors (Gerrard et al., 2005). More recently a small molecule BMP antagonist dorsomorphin has also been shown to block BMP signaling and has been used to promote cardiomyogenesis (Hao et al., 2008).

The primary goal of this work is to elucidate the role of BMP on germ cell formation in hESC and hiPSC. We hypothesized that BMP4 would be required for PGC formation in both hESC and hiPSC. Additionally, we wanted to examine the effect of co-induction with other BMP signaling factors, such as BMP7 and BMP8 on PGC formation; given synergistic effects demonstrated in mice models.

We also explored the effect of increasing the most significant signaling factor identified in our induction treatments, also called a boost treatment (Goldman et al, 2009). The goal of using boost treatments was to enhance PGC induction efficiencies. In order to quantitatively evaluate the efficiency of PGC induction following BMP treatments and identify the most significant factor for boost treatments, a time-course experiment was performed using the following BMP treatments in HES media without bFGF:

1) BMP4

2) BMP7

3) BMP8

4) BMP4 and BMP7

5) BMP4 and BMP8

6) BMP7 and BMP8

7) BMP4, BMP7 and BMP8.

The time-course evaluated the expression of BLIMP1 following four and five days of BMP treatment. The experiment was also used to determine the timepoint for the initiation of BLIMP1 expression following BMP treatment. It additionally provided data for quantitative analysis to determine if co-induction of BMPs is significantly more effective than unaccompanied BMP treatments. Quantitative data was gathered by determining the percentage of cells expressing BLIMP1 as well as real-time Q-PCR to determine relative gene expression levels specifically expressed in PGC.

The inhibition of BMP signals on the expression of BLIMP1 while all other culture conditions are kept constant was also evaluated. The small signaling molecule dorsomorphin (DM) was added to differentiation media subjected to the induction pressures of BMP treatments. Immunocytochemistry was used to determine if inhibition of BMP signals, by receptor antagonist dorsomorphin interrupts the activation of BLIMP1 and ultimately the PGC fate.

Once the highest efficiency induction strategy for deriving PGC was determined, research aimed to define a reliable method of collecting PGC from the heterogeneous cultures. Several cells surface markers of PGC have been described, including cluster of differentiation 117 (CD177), C-X-C chemokine receptor type 4 (CXCR-4), and stage specific embryonic antigen 1 (SSEA1) (Xiang-long et al., 2005; Geijsen et al., 2004; Molyneaux et al., 2003; Knaut et al., 2000). Precision identification of PGC by cell surface markers was pivotal to isolation studies and contributed in the determination of an optimal protocol for derivation and isolation of PGC from pluripotent cultures.

Determining the Specific Transcriptional Regulator of the Germline

Mouse studies have served as an archetype for identifying genes specifically expressed in the germline; this is because very few studies examine human germline formation. Dynamic global gene expression of PGC identified PGC+/ESC- germ cell markers TNAP, BLIMP1, Stella and Fragillis (Sabour et al., 2011; Ohinata, 2005). BLIMP1 is the paradigm marker for early identification of

PGC and has been functionally characterized as the transcriptional regulator of the germline (Figure 2).

BLIMP1 expression is critical for the formation of PGC, acting as a transcriptional regulator for the initiation of the germline (Ohinata 2009; Kurimoto, 2008; Ohinata, 2005; Vincent, 2005). Repression of somatic genes, especially the HOX gene cluster, is highly associated with BLIMP1 expression. Repression of the HOX cluster is important to preventing mesoderm differentiation, experienced by PGC somatic neighbors. BLIMP1 deficient PGC are not capable of repressing the somatic program, which abruptly halts PGC specification. To a lesser extent, BLIMP1 impairment leads to lower expression levels of PGC specific genes (Kurimoto et al., 2008). Following BLIMP1 expression, PGC should initiate the expression of Stella and Fragillis and maintain pluripotency gene expression of OCT4, Sox2, Nanos3 and Nanog (Ohinata et al., 2009).

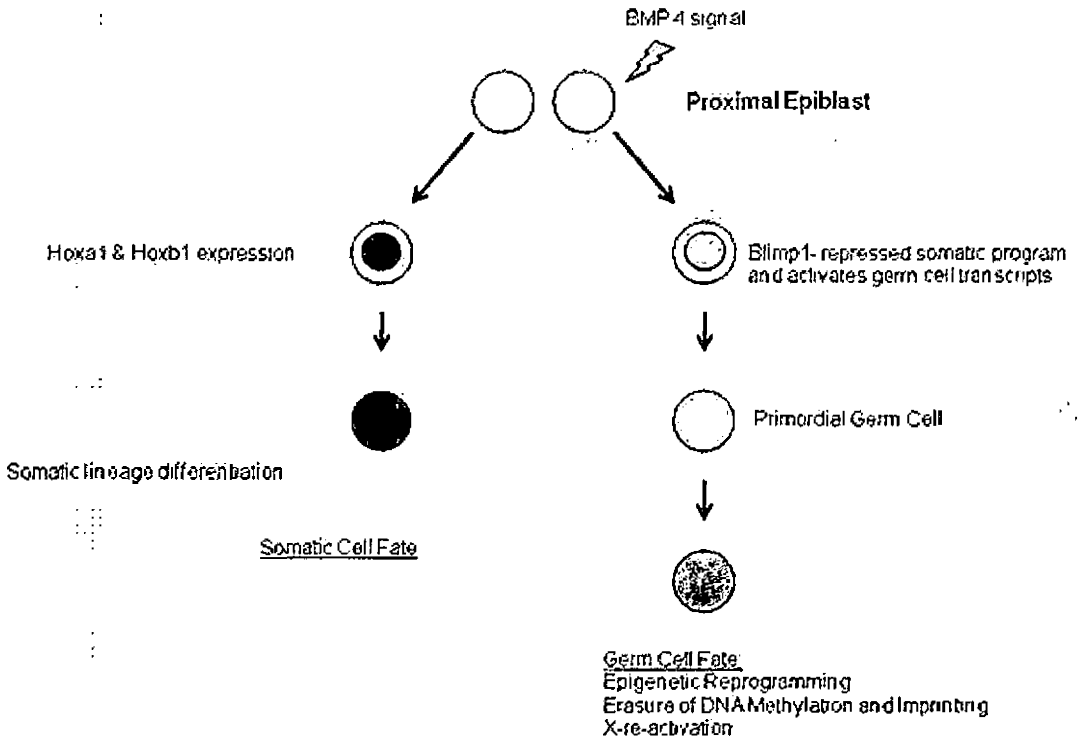

Figure 2. Primordial Germ Cell Specification Program. BLIMP1 expression, following BMP signaling, is responsible for somatic program repression, upregulation of other PGC markers and complete epigenetic reprogramming.

There are two major variances of BLIMP1 that have been identified. The full-length transcript, BLIMP1a, has been associated with normal function in B-lymphocytes but the shorter variance, BLIMP1b, has been related to B-cell oncogenesis. Given the correlation of BLIMP1b expression and oncogenesis, BLIMP1a was hypothesized to be the variance responsible for the transcriptional regulation in early PGC formation. The effects of BLIMP1 variances during hESC and hiPSC differentiation were analyzed in order to study the effects of BLIMP1a and BLIMP1b. Once BMP treatments were confirmed to induce PGC

specification, transcripts of BMP-induced cultures were probed for the expression of BLIMP1a and BLIMP1b. Additionally, a Tet-On transfection system was utilized to promote the over-expression of each variance for comparative analysis. The effect of BLIMP1 variance over-expression was determined using real-time Q-PCR and single cell real-time Q-PCR.

Observing Early Epigenetic Changes in the Germline

Studies concerned with the dynamics of epigenetic reprogramming in the mouse germline have identified two significant changes of histone protein 3 that occur in concert with genome-wide DNA demethylation. Epigenetic reprogramming is postulated to be essential for the reacquisition of totipotency during germline formation, and removal of the previously established epigenetic memory. (Seki et al., 2007; Seki et al., 2005)

Research will focus on the changes in histone 3 lysine markers during germ cell differentiation in hESC and hiPSC. Given the significance of epigenetic reprogramming during germline formation, it is expected that the patterns of histone modification demonstrated in mice will be evolutionarily conserved in human germ cells. In order to establish the changes in histone methylation markers of interest, immunocytochemistry analysis was performed on undifferentiated pluripotent cells, spontaneously differentiating cells and PGC-induced cells.

CHAPTER TWO

LITERATURE REVIEW

The Germline

The germline is a significant lineage, responsible for the propagation of the parental genome to subsequent generations. Primordial germ cells (PGC) are the founder population of the germline (Figure 3).

Figure 3. OCT4-Enhanced Green Fluorescent Protein Primordial Germ Cells. Migrating along the genital ridge of day 12 mouse embryo. (Courtesy of Duncan Liew,)

Of the more than two hundred cell types described in the human body, germ cells are the only cell type that undergoes meiosis in order to produce haploid cells for sexual reproduction. The germline has been referred to as the one of the few cell types capable of achieving totipotency (Mitalipov et al, 2009). PGC in the developing embryo will mature into gametes, which fuse in sexual reproduction to form a zygote. The zygote will divide and develop to form every cell of the new organism including the germ cells as well as supportive extraembryonic tissues.

Early PGC are difficult to discriminate from hESC due to the co-expression of pluripotency markers such as alkaline phosphatase (ALP) and OCT4 (Ginsburg, 1990; Yeom et al., 1996). However, as normal embryonic development continues hESC begin to differentiate into somatic cell lineages and only the germ line will continue to express OCT4 and maintain pluripotency (Yeom, 1996). The avoidance of somatic lineage differentiation and maintenance of pluripotency during germ cell development provides a unique developmental model.

Theories of Germline Specification

In 1885, Weismann postulated that germline specification occurs as a result of determinants passed down from the previous generation (Weismann et al, 1885). Later known as preformation, asymmetrical localization of maternally inherited determinants is responsible for designating germline cells, this mode of germ cell specification holds for model organisms such as *Caenorhabditis*

elegans, Drosophila melanogaster, Xenopus laevis, and *Danio rerio* (Wylie, 2000; Eddy, 1978).

However, attempts to identify preformation determinants in mammalian oocytes demonstrated that the preformation mode of germ cell specification is not ubiquitous (Eddy et al,1981). In the majority of metazoans and all mammals, the germ cell specification mode utilized is called epigenesis. During epigenesis naïve cells, capable of differentiating into either germ cells or mesoderm lineages, will be restricted to the germline by signaling molecules received from neighboring cells (Extavour et al., 2003; Johnson et al., 2003).

Germ Cell Formation

Germ cell formation can be divided into four main stages (Figure 4):

1) Specification

2) Migration

3) Colonization

4) Maturation

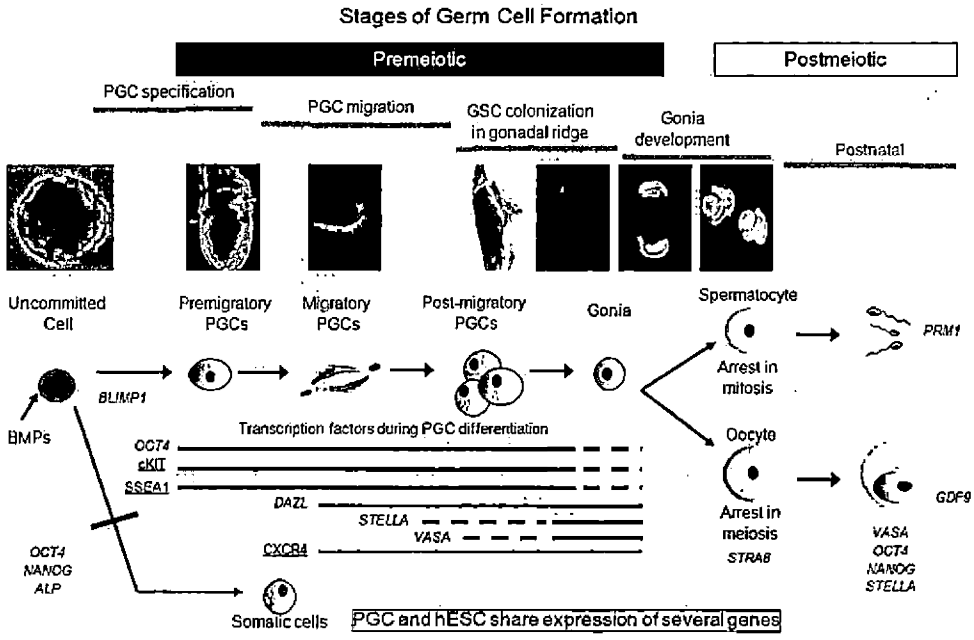

Figure 4. An Overview of Primordial Germ Cell Formation. Major stages include specification, migration, colonization, and development. The development stage occurs during prenatal and postnatal timepoints. Patterns pre-meiotic of gene expression are below each stage. (Courtesy of Dr. Duncan Liew, University California Riverside Stem Cell Core)

Specification. The mouse model has been the archetype for determining molecular interactions within the mammalian embryo that result in the specification of PGC, the founding population of the germline. Extensive *in vivo* studies of mouse embryonic development have led to the following mammalian paradigm of germ cell formation. During embryonic development, a group of cells proximal to the primitive streak elude normal somatic programming during early gastrulation (Lanza, 2009). The cells are located within the posterior epiblast, and receive molecular signaling from surrounding mesoderm cells. Bone morphogenetic proteins (BMPs) have been identified to be the critical factor

to induce PGC formation in the early mouse embryo (Dudley et al., 2010; Lawson et al., 1999). BMP signals initiate a cascade of molecular interactions that produce germ cells (de Sousa Lopes, 2004; Toyooka et al., 2003;). Furthermore, BMP signaling has been demonstrated to result in the expression of the master regulator of the germline, B-lymphocyte maturation protein 1 (BLIMP1) (Ohinata, 2009).

Migration. The onset of BLIMP1 expression initiates transcriptional changes which repress the somatic cell program and upregulate germ cell genes (Kurimoto, 2008; Ohinata 2005). PGC were first identified as an alkaline phosphatase (ALP)-expressing niche within the proximal, posterior epiblast. The pre-migratory primordial germ cells will begin to proliferate and continue to grow in cell number until the niche has grown by 10-fold. At this point PGC will mature to migratory PGC and emerge from the extraembryonic mesoderm (Lawson, 1994; Ginsburg et al., 1990). Migratory PGC will propagate and mature during migration though the primitive hindgut and dorsal mysentery. Survival and proper migration rely on the regulation by CXCR-4 signaling (Molyneaux et al., 2003).

Colonization. Migratory PGC further mature into post-migratory germ cells shortly after entering the genital ridges of the gonads (Tam and Snow, 1981). Once germ cells have colonized the gonads the presence of the Sry gene encoded on the Y sex chromosome will determine the sexual identity of the germ cells. (Lanza, 2009)

Maturation. In the genital ridges the germ cells will revert to a pre-meiotic cell cycle, and initiate meiosis via retinoic acid signaling from the adjacent mesonephros. The expression of the Sry gene product will curb male germ cells from the default meiotic pathway experienced by female germ cells. Female germ cells experience permanent mitotic arrest prior to birth and enter prophase I shortly after, meiotic female germ cells pause during diplotene stage of Prophase I and await menarche for continued meiosis. Conversely, male germ cells enter G1/G0 mitotic arrest, and Sry downstream targets inhibit meiosis and promote support from surrounding somatic Sertoli cells. After birth prespermatagonia will begin spermatogenesis and await meiosis following puberty. (Lanza, 2009)

Bone Morphogenetic Protein Signaling as a Mechanism to Promote Primordial Germ Cell Specification

BMP signaling in the mouse embryo has been identified as an essential requirement of inducing the expression of BLIMP1, an early PGC marker (Ohinata, 2009). In 2009, Ohinata demonstrated that BMP4 alone is capable of inducing germ-like cells from the developing epiblast mouse. Gene knockout studies demonstrated that BMP4 initiates BLIMP1 transcription through transforming growth factor beta (TGFb) signaling.

BMP, a member of the TGFb superfamily, will initiate an intracellular cascade that works in combination with another TGFb cascade, which is highly active and initiated by activin. BMP signaling is initiated by BMP ligand binding to a heterodimer receptor complex (Figure 5). The receptor complex consists of two

constitutively active type II receptor subunits and two type I receptor subunits which are actively recruited by the ligand. The activated receptors of TGFb signaling will possess serine/threonine kinase activity, which will initiate phosphorylation cascades (Itman et al, 2006).

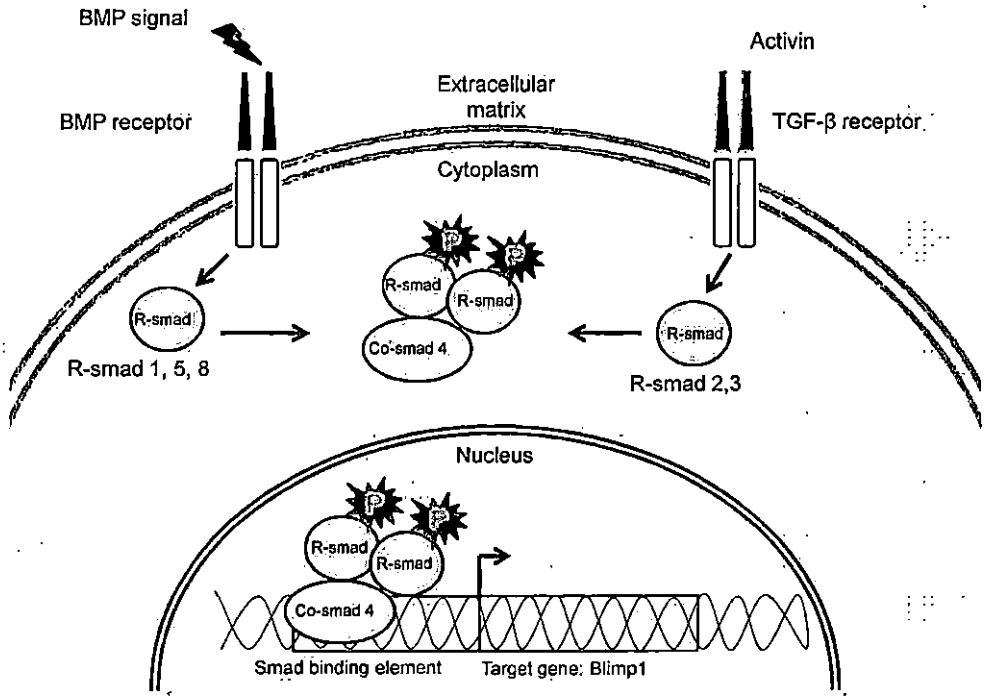

Figure 5. Transforming Growth Factor Beta Signaling by Smad Proteins. BMP4 binds to BMP receptors which activate the formation of a smad protein complex, co-localization permits nuclear translocation and subsequent transcriptional modification. (Itman et al., 2006).

Accordingly, extracellular binding of BMP4 ligand to constitutively active activin receptor-like kinase (ALK) 1/6 will be followed by the recruitment of the

bone morphogenetic protein receptor II (BMPRII) dimer, forming the complete heterdimer complex. BMP4 binding of the heterodimer complex will initiate intracellular kinase activity which will phosphorylate receptor activated-smads (R-Smads) 1, 5 and 8. The activated R-Smads will associate with co-Smad4, which has a nuclear localization sequence. Accordingly, the BMP ligand initiated signaling is translocated to the nucleus to promote the transcription of BLIMP1. Thus, prevailing evidence supports the role of BMP4 as the ligand initiator of BLIMP1 expression and PGC specification. (Ohinata et al., 2009)

The effect of BMPs that are structurally heterogeneous from BMP4 has also been previously examined. Co-localized expression of BMP4 and BMP8 has been demonstrated in the murine model. Although BMP4 initiates the expression of BLIMP1 through TGFb type receptors, BMP8 does not directly affect BLIMP1 expression as it doesn't act via TGFb signaling. However, BMP8 does play a role in counteracting inhibitory signals that act to prevent germ cell specification. Thus the synergistic effects of BMP4 in concert with other BMP signals has been documented (Ohinata et al, 2009).

Function of B-Lymphocyte Induce Maturation Protein1 During Primordial Germ Cell Specification

BLIMP1 has been well documented as a transcriptional regulator directing the repression of promoter regions. As a transcriptional repressor the function of BLIMP1 in several cell lineages is to restrict differentiation to a specific cell type. In retinal differentiation BLIMP1 prevents bipolar cell fate and accordingly

promotes the differentiation of photoreceptor cells (Brzezinski et al., 2010). During epidermal multipotent stem cell commitment the expression of BLIMP1 promotes sebaceous gland progenitors with self-renewing characteristics (Horsley et al, 2006). BLIMP1 was first identified in B-lymphocyte maturation (Gyory et al., 2003). Thus it is apparent that BLIMP1 can perform many roles as a transcriptional repressor and affects the differentiation of several cell types, when expression occurs during the appropriate windows of time. Previously discussed expression-windows of BLIMP1 occur during late stages of cell lineage differentiation. However, when BLIMP1 expression is initiated in naïve uncommitted cells in the early mouse embryo, BLIMP1 will direct hESC toward the germline.

BLIMP1 belongs to the positive regulatory domain zinc finger (PRDM) protein family of transcriptional repressors, characterized by positive regulatory and zinc finger binding domains. Like other PRDM genes, BLIMP1 (PRDM1) transcription can results in the expression of two distinct variances, BLIMP1a and BLIMP1b. The gene sequence possesses two ATG transcription start sites (Figure 6). The BLIMP1a transcript consists of seven exons, which encode the full-length 798 amino acid protein. Alternatively, a novel transcription start site for BLIMP1b is located 155 base pairs upstream of the fourth exon. Thus BLIMP1b will only encode the last four exons of BLIMP1a and the resulting protein consists of 697 amino acids. Accordingly, the variances share a common carboxyl-terminus and differ in their amino-terminus. Loss of the first 101 amino acids of

the full length BLIMP1a protein disrupts the function of the positive regulatory domain of the BLIMP1b. (Gyory et al., 2003)

Comparative examination into the roles of these variances in B-lymphocyte differentiation has revealed an important distinction between the two variances of BLIMP1. Myeloma and transformed cell lines undergoing B-lymphocyte differentiation expressed high levels of BLIMP1b. Conversely, BLIMP1a was determined to be prominent and highly expressed in normal B-lymphocyte maturation (Gyory et al., 2003). The identification of the primary variances responsible for the functional role in PGC specification remains to be elucidated.

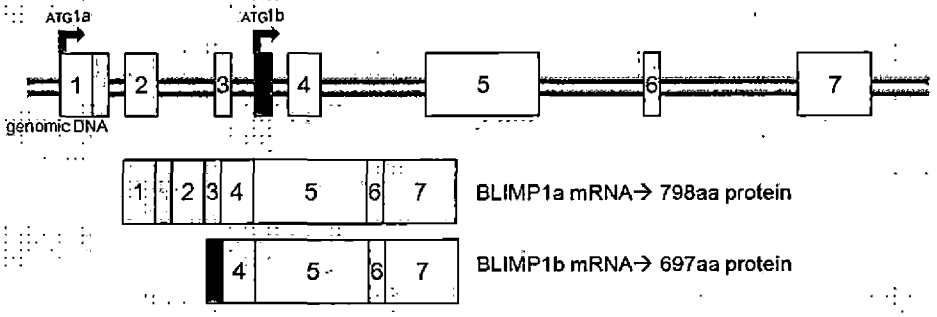

Figure 6. B-Lymphocyte Induced Maturation Protein1 Variance Exon Map. The variances result from two ATG transcriptional start sites and result in protein product of different amino acid lengths. BLIMP1a is a 798 amino acid protein, and BLIMP1b is a 697 amino acid protein.

Epigenetic Properties of Germ Cells

Epigenetic erasure is a hallmark of PGC formation, and a pathway that is unique compared to all other somatic cell lineages. Epigenetic patterns determine the accessibility of specific regions of DNA, providing variations in cellular phenotypes. DNA accessibility is determined by the status of the chromatin. Changes in chromatin conformation will cause changes in the transcriptional state of the DNA structure. Chromatin can be modified in two ways, the DNA sequence can be modified or the histone proteins which the DNA wraps around can be modified. DNA can be methylated in order to directly silence genes. Furthermore, DNA can be indirectly silenced by further condensing DNA around histone proteins. The histone code is the modified conformation of histone proteins, which can be modified by protein subunit interchange and amino acid methylation, deacetylation, ubiquitylation or sumoylation. Heterochromatin is associated with a non-transcriptionally active DNA, whereas euchromatin is transcriptionally active. Germ cells must initiate the erasure of the aforementioned epigenetic changes prior to gamete formation so that the zygote will be free of epigenetic marks. Germ line epigenetic reprogramming permits the reestablishment of totipotency. Additionally, epigenetic reprogramming removes genomic imprinting, or parent specific silencing of particular genes, so haploid gametes can establish new imprinting patterns following fertilization. (Lanza, 2009)

Mouse modeling has been used to describe the epigenetic changes of the developing mammalian embryo, given the consequences of improper epigenetic reprogramming the patterns of these changes should be evolutionarily conserved. Mouse studies have identified two significant histone methylation patterns that correlate with genome-wide DNA demethylation (Seki et al., 2007; Seki et al., 2005). Modification of histone 3 via dimethylation of lysine 9 (H3K9me2) and the trimetylation of lysine 27 (H3K27me3) are methylation marks that undergo changes dependent on germ cell maturation. Epigenetic reprogramming was proposed to occur progressively as PGC begin to migrate, as observed by the downregulation of H3K9me2 and concomitant upregulation of H3K27me3 (Figure 7).

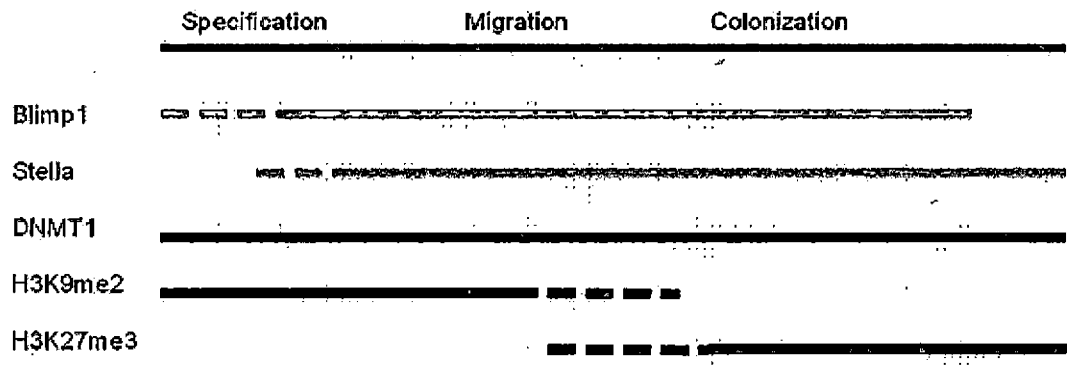

Figure 7. Germline Epigenetic Reprogramming Patterns in Mice. Specification is initiated by the expression of BLIMP1, after which other germline genes like Stella are upregulated. Epigenetic reprogramming involves genome-wide DNA demethylation by DNA methyltransferases, like DMNT1. Two histone 3 modifications associated with DNMT1 expression are the repression of histone 3 lysine 9 dimethylation (H3K9me2) and the upregulation of hisone 3 lysine 27 trimethylation (H3K27me3).

Derivation Of Germ Cells From Human Pluripotent Stem Cells

Haploid gametes have been derived from male and female mESC albeit at very low efficiency (Kehler et al., 2005). Spontaneous differentiation enabled by embryoid body (EB) formation was the method primarily utilized to induce germline formation to sperm and oocyte (Geijsen et al., 2004; Hubner et al., 2003). Improving upon foundational mouse research by formulating induction and isolation strategies has enhanced efforts to derive and manipulate functioning human germ cells *in vitro*. The primary approach to deriving human germline *in vitro* focuses on isolation at specific stages of germ cell formation. Accordingly, several cell surface markers of the germline have been described and used to isolate germ cells (Xiang-long et al., 2005; Geijsen et al., 2004; Knaut et al., 2003; Molyneaux et al., 2003). A therapeutic goal of human germline studies is to derive patient specific gametes for millions world-wide who suffer from infertility. Toward this effort, human meiosis has been recently achieved *in vitro* by long term differentiation of heterogeneous cultures, but their efficiency and functionality remains to be fully investigated (Eguizabal et al., 2011).

CHAPTER THREE

METHODOLOGY

Culture Techniques

Culture of hESC and hiPSC

To maintain hESC and hiPC cultures, H9 hESC and Riv9 hiPSC were plated into BD Falcon polytene tissue culture treated plastic which has been additionally coated with Geltrex (1:100; Invitrogen). H9 hESC and Riv9 hiPSCs were fed serum-free defined mTeSR1 media (Stem Cell Technologies) containing 100 ng/ml basic fibroblastic growth factor (bFGF) daily and maintained in an environment of 5% CO2 at 37°C. Cells were passaged every five to seven days when they had reached 80-90% confluency. Cells were split using accutase (Innovative Cell Technologies Inc.) and mechanical disaggregation with 3 mm glass beads (Fisher Brand) followed by dilution and collection using Dulbecco's modified eagle medium (DMEM).

Differentiation of Primordial Germ Cells from hESC and hiPSC Cultures

PGC differentiation was initiated when cells were 50-80% confluent. On day zero of BMP induction experiments the daily media was changed to human embryonic stem cell (HES) media without bFGF. HES media stock contained 400 ml knockout DMEM (Invitrogen), 100 ml knockout serum replacement (KOSR) (Invitrogen), 5 ml 1X glutamax, 5 ml non-essential amino acid solution (NEAA), 14 µl 2-B-mercaptoethanol (BME) ± basic fibroblastic growth factor (bFGF). HES

media without bFGF was supplemented with BMP signaling factors. Based on preliminary data BMP4 was supplemented at a higher concentration in subsequent experiments, 100 µg/ml; compared to BMP7 and BMP8 supplemented at a concentration of 50 µg/ml.

Magnetic Activated Cell Sorting of Primordial Germ Cells

Differentiated BMP-induced PGC were treated with rho kinase inhibitor (RI), washed with PBS and trypsinized with 0.25% EDTA Trypsin (Life Technologies). Cell pellets were then resuspended in 500 µl cold Magnetic activated cell sorting (MACS) buffer (Miltenyi Biotec) and cell surface antibody, CD117, CXCR4 or SSEA1 at appropriate dilutions (Table 1). Cells were then stained for one hour at 4°C. Cells were washed and resusupended in 500 µl MACS buffer and incubated an additional hour with magnetic beads specific to primary antibodies. Prior to MACS by the Auto MACS Pro (Miltenyi Biotec), the magnetic columns were changed and cells were washed and resuspended in 3 ml of cold MACS buffer. Positive and negative cell fractions for CD117, CXCR4 or SSEA1 were then collected into labeled 15 ml conical tubes using the Possel_s MACS isolation protocol. Cell pellets from positive and negative fractions were spun down and stored at -80°C for subsequent molecular biology.

Table 1.Primary Antibody Dilutions

Antibody	Dilution Ratio	Supplier
BLIMP1	1:200	Cell Signal
Oct-4	1:100	Santa Cruz
CXCX-4	1:10	R & D Systems
CD117	10 µl / 1,000 cells	Millipore
SSEA1	1:100	Millipore
H3K9me2	1:100	Novus Biologicals
H3K27me3	1:250	Millipore

Molecular Biology

RNA Extraction and Reverse Transcription

After cell pellets were isolated from a sample they were stored at -80°C prior to RNA extraction. Once thawed, the cell pellet was lysed and RNA extracted according to the Bio-Rad RNA extraction kit (Bio-Rad). The concentration of the RNA was measured using an Epoch micro-plate spectrophotometer and Take3 micro-spot plate (BioTek). The first-strand cDNA synthesis was accomplished by using the iScript cDNA Synthesis kit (BioRad), after which reverse transcription polymerase chain reaction (RT-PCR) was used to amplify the cDNA. Each RT-PCR reaction consisted of PCR master mix, sample cDNA and 1 µl each of both the forward and reverse primers of genes of interest (Table 2). RT-PCR amplifications were initiated at 95°C for 5 minutes (mins) followed by annealing and extension.

Table 2. Real Time-Polymerase Chain Reaction Oligonucleotide Primers

Gene	Forward Sequence (5'-3')	Reverse Sequence (5'-3')
BLIMP1a	CAT GGA GGA TGC GGA TAT GAC	AGT GGT GGA GGA TGG AAT GG
BLIMP1 b	GGA AAG ATC TAT TCC AGA	AGT GGT GGA GGA TGG AAT GG
BLIMP14	AAC AAA CAC ATG CGA GTC CA	CTC CCA AAG TGC TGG GAT TA
ACTIN b	ATC TGG CAC CAC ACC TTC TAC AAT GAG CTG CG	CGT CAT ACT CCT GCT TGC TGA TCC ACA TCT GC

Real-Time Quantitative Polymerase Chain Reaction

Real-time Q-PCR was performed using a 384-well real-time thermocycler (BioRad), and samples were repeated in duplicate. Each reaction consisted of 2.5 µl IQ Supermix (BioRad), 0.25 µl gene specific Taqman probes (Applied Biosystems) (Table 2), 1.25 µl distilled water and 1 µl diluted cDNA (standardized based on housekeeping gene controls). PCR amplifications were initiated at 95°C for 10 mins followed by 42 cycles of 95°C for 15 seconds and 60°C for 60 seconds. The Real-time Q-PCR data were analyzed using the comparative C_T method.

Table 3. Taqman Probes for Real-Time Quantitative-Polymerase Chain Reaction

Gene	Accession Number	Assay ID
ACTIN B	NM_001101.3	Hs 99999903_m1
GAPDH	NM_002046.3	Hs99999905_m1
18 S	18s_consensus.0	Hs99999901_s1
BLIMP1	NM_001198.3; NM_182907.1	Hs00153357_m1
OCT4	NM_001173531.1	01895061_m1
NANOG	NM_024865.2	Hs02387400_g1
VASA	NM_001142549.1	Hs00987125_m1
STELLA	NM_199286.2	Hs01931905_g1
DAZL	NM_001190811.1	Hs00154760_m1
KIT	NM_000222.2	Hs00174029_m1
BRACHYURY	NM_003181.2	Hs00610080_m1
CDX 2	NM_001265.3	Hs01078080_m1
SOX 17	NM_022454.3	Hs00751752_s1
GSC	NM_173849.2	Hs00418279_m1
HOXB1	NM_002144.3	00157973_m1

Single Cell Real-Time Quantitative Polymerase Chain Reaction

Cells for single-cell real-time Q-PCR were sorted directly into a 9 µl lysis solution plus 1 µl DNAase (Ambion) in a tissue culture treated flat bottom 96 well plate (BD falcon). Cell lysis was stopped after 5 minutes by the addition of 1 µl of stop solution (Ambion). Total cell lysate was then directly added to 4.5 µl VILO RT master mix (Ambion), containing 3 µl of VILO RT mix and 1.5 µl SuperScript RT enzyme. PCR amplifications were initiated at 25°C for 10 mins followed by of 42°C for 60 mins and 85°C for 5 mins. Single cell real-time Q-PCR data were analyzed using the comparative C_T method.

Immunocytochemistry

Cells were washed twice with phosphate buffered saline (PBS) without calcium or magnesium, and then fixed with 4% paraformaldehyde for 10-15 minutes. The cells were subsequently blocked using an antibody staining solution (ASS) of 99% PBS without Ca^{2+} or Mg^{2+}, 1% goat serum and 0.1% triton-X. Primary antibodies were diluted (Table 1) in ASS and were incubated overnight at 4°C. The following day primary antibodies in ASS were removed and the cells were washed twice with ASS. Next the secondary antibodies (diluted at a ratio of 1:500 in ASS) were added and left to incubate at 25°C in the dark. Following secondary staining the cells were again washed twice with ASS followed by one PBS without calcium or magnesium rinse. Finally the cells were mounted with glycerol and Vectashield mounting medium with DAPI (Vector Labs), and

subsequently imaged using a Nikon Ti Eclipse microscope and NIS3.2 Elements software.

Genetic Manipulation

Plasmid Preparation

Transformation of competent *Escherichia coli* (Invitrogen) was accomplished by thawing competent cells stored at -80°C. Once thawed 1-5 µl of plasmid (pCAG-rtTA, pTRE-BLIMP1a, pTRE-BLIMP1b, or pTRE-GFP) was added to the competent cells, mixed, and incubated on ice for 20 minutes. Competent cells were then heat shocked at 45°C for 1 minute and immediately placed on ice again for two minutes. Competent cells that had taken up the plasmids were then cultured in 1 ml of ampicillin-containing Terrific broth (AMP-TB) (Invitrogen) for one hour. The bacteria were then streaked using plastic loops onto agar containing AMP (Invitrogen) in Petri dishes and stored in an environment of 5% CO2 at 37°C for 24 hours.

Single bacterial colonies were isolated for culture and grown in AMP-TB in suspension at 220 rpm and 37 °C; 8 hours in 5 ml culture, and then transferred to 200 ml culture for 16-18 hours. Following bacterial suspension culture, cell pellets were collected by centrifugation at 3,500 rpm at 4°C for 30 minutes. The cell pellets were then frozen at -20°C. Plasmids (pCAG-rtTA, pTRE-BLIMP1a,

pTRE-BLIMP1b, or pTRE-GFP) were isolated from the bacterial pellets using the Pure Yield Maxiprep system (Promega).

Nucleofection

hESC were transfected with a Tet-On system using co-nucleofection. Cells were treated with rock inhibitor (RI) at a concentration of 10 µg/ml for at least one hour prior to nucleofection to prevent cell death. Cells were then washed with PBS without calcium and magnesium and then disassociated into single cells using 0.25% trypsin/EDTA (Invitrogen). Cells were collected in MEF media (450 ml DMEM, 50 ml fetal calf serum (FCS), 5 ml 1X glutamax, 5 ml NEAA, and 5 ml 1X sodium pyruvate) and centrifuged at 800 rpm for 3 minutes. Each cell pellet was resuspended in 100 µl of pre-warmed human stem cell nucleofector solution 1 (Lonza) and transferred into a nucleofector cuvette. Then, 1 µg of expression vector pCAG-rtTA and 20 µg of one of the bi-directional response vectors pTRE-BLIMP1a, pTRE-BLIMP1b, or pTRE-GFP was added to the cells in human stem cell nucleofector solution 1. The cuvette was then swirled and taped twice on a hard surface before being placed into the cuvette holder of the Lonza Amaxa Nucleofector II Device. Nucleofection program B-16 was run to introduce the plasmids to the cells' nucleus. Following nucleofection, cells were removed from the nucleofector cuvette and placed in a 1.5 ml Eppendorf tube containing 1 ml of pre-warmed conditioned HES media with bFGF supplemented with RI to prevent further cell death. Cells in conditioned

HES media were incubated in 5% CO2 at 37°C for 10 minutes after which they were plated drop-wise onto irradiated mouse feeders. (Chatterjee, 2011)

Clones that were successfully nucleofected were selected based on puromyocin resistance genes in the plasmids over a period of two to four weeks. Once colonies were capable of surviving in antibiotic selection at a ratio of 1:1000 they were picked. Colonies were manually picked using a 200 µl pipette and split into two wells of a 24 wells plate, one of which was immediately induced by the addition of doxycycline (Dox). Following 24-hour Dox induction the Nikon Ti Eclipse microscope was used to confirm stable transfection.

Induction of B-Lymphocyte Induced Maturation Protein1 Variances

hESC expressing either BLIMP1a or BLIMP1b were fed serum-free defined mTeSR1 media (Stem Cell Technologies) containing 100ng/ml bFGF daily and maintained in an environment of 5% CO2 at 37°C. When cells were 70% confluent the media was changes to HES without bFGF and the Tet-On system was induced by adding Dox (1:1000). Cells were induced to express either BLIMP1a or BLIMP1b for one day, after which cells were disassociated using accutase and mechanical disaggregation with 3mm glass beads followed by dilution and collection using DMEM. Cell pellets were stored at -80°C for RNA extraction, RT-PCR and real-time Q-PCR analysis. The Tet-On overexpression of BLIMP1a and BLIMP1b was also induced for three days, after which fluorescent activated cell sorting (FACS) was used to isolate single cells for single cell real-time Q-PCR.

Fluorescent Activated Cell Sorting

Prior to delivering cells to the FACS technician cultures were: washed with PBS without calcium or magnesium, then disassociated into single cells using 0.25% trypsin/EDTA. Following inactivation with MEF media cells were centrifuged at 800 rpm for 3 min. The cell pellet was resuspended in 500 µl PBS + 0.1% fetal bovine serum (FBS) and kept on ice until the sample was sorted. Once sorted, the positive and negative cell fractions were collected separately and RNA was immediately extracted.

Image-J Analysis

Image-J was used to analyze data in two ways. The cell counter function was used to quantify the immunocytochemistry images taken with the Nikon Ti Eclipse on the 10X magnification. The counter keeps track of each cell clicked in an image, so that the number of cells expressing a protein of interest is quantified.

Additionally, Image-J intensity function was used to quantify the expression intensity of 10X magnification images taken with the Nikon Ti Eclipse. With this function the expression level of two different proteins, for which immunocytochemistry had been perform, could be compared to establish correlation patterns.

Statistical Data

Experiments were carried out in duplicate culture wells which contained an average of 500,000 cells. Quantitative data is presented as standard deviation from mean values. Statistical significance was determined by Student's t-test with $p<0.05$ as a threshold for significance.

CHAPTER FOUR

RESULTS

Bone Morphogenetic Protein4 Induced Primordial Germ Cell Specification From Human Pluripotent Stem Cells

Time-course examination was performed to determine the timepoint following BMP treatment that resulted in PGC induction, as determined by expression of master regulator BLIMP1. Additionally, time-course examination was designed to determine whether co-induction of BMP signals exert synergistic effects on PGC formation. Similarly the time course quantitatively compared multiple BMP co-induction efficiencies to determine the best induction strategy for PGC specification. In order to measure and analyze the induction of PGC formation both H9 hESC and Riv9 hiPSC were grown to 70% confluence and then changed from daily mTeSR media to HES differentiation media supplemented with 50 µg/ml BMP. Treatments included BMP4; BMP7; BMP8; BMP4 & 7; BMP4 & 8; BMP7 & 8; and BMP4, 7 & 8.

Following one, three, and five days of differentiation the H9 hESC and Riv9 hiPSC were fixed for immunocytochemistry analysis of pluripotency marker OCT4 and PGC specific BLIMP1 protein expression (Figures 8, 9 and 10). BLIMP1 was not expressed following one day of BMP induction. Similarly, immunocytochemistry analysis also revealed that three days of BMP induction was not sufficient to induce BLIMP1 expression. BLIMP1 expression was detected after five days of BMP treatment.

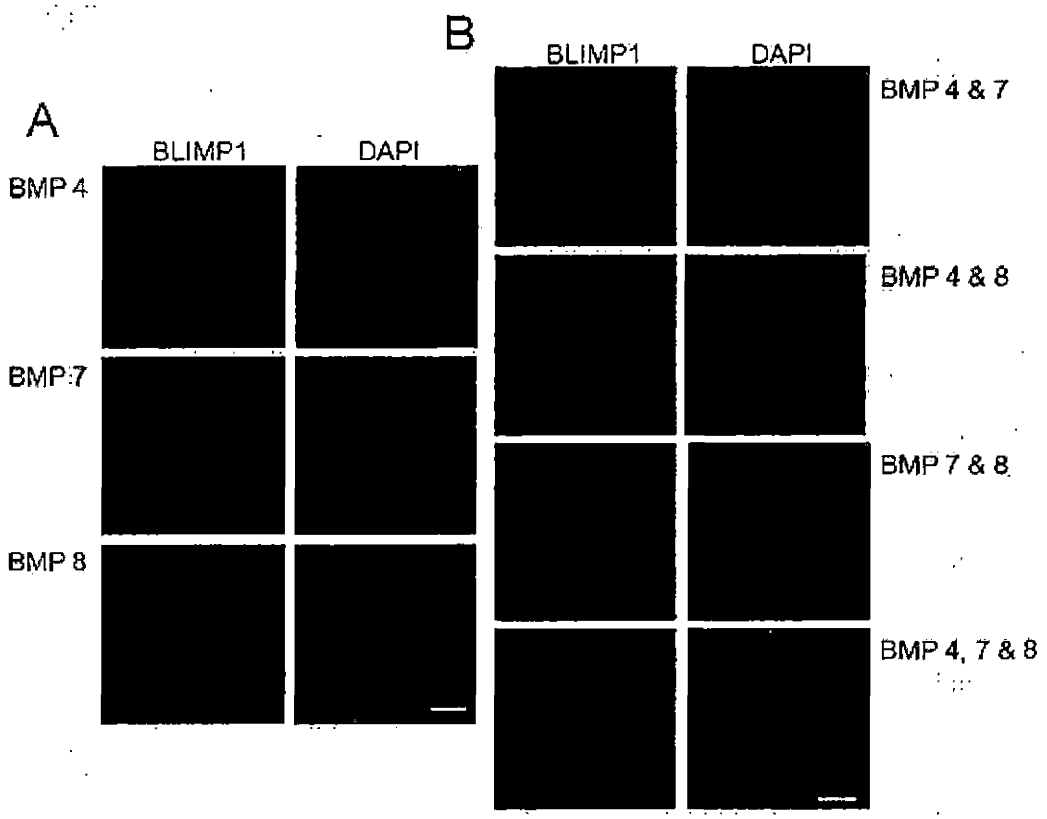

Figure 8. Day Three Immunocytochemistry Analysis of H9 hESC Bone Morphogenetic Protein Treatments. (A) Immunocytochemistry analysis of BMP4, BMP7 and BMP8-treated H9. BLIMP1 expression was not detected. (B) Co-induction using BMP4 & 7, BMP4 & 8, BMP7 & 8, and BMP4, 7 & 8 also did not appear to promote BLIMP1 expression on day three. Representative images taken at 10X. Scale bar = 50 microns.

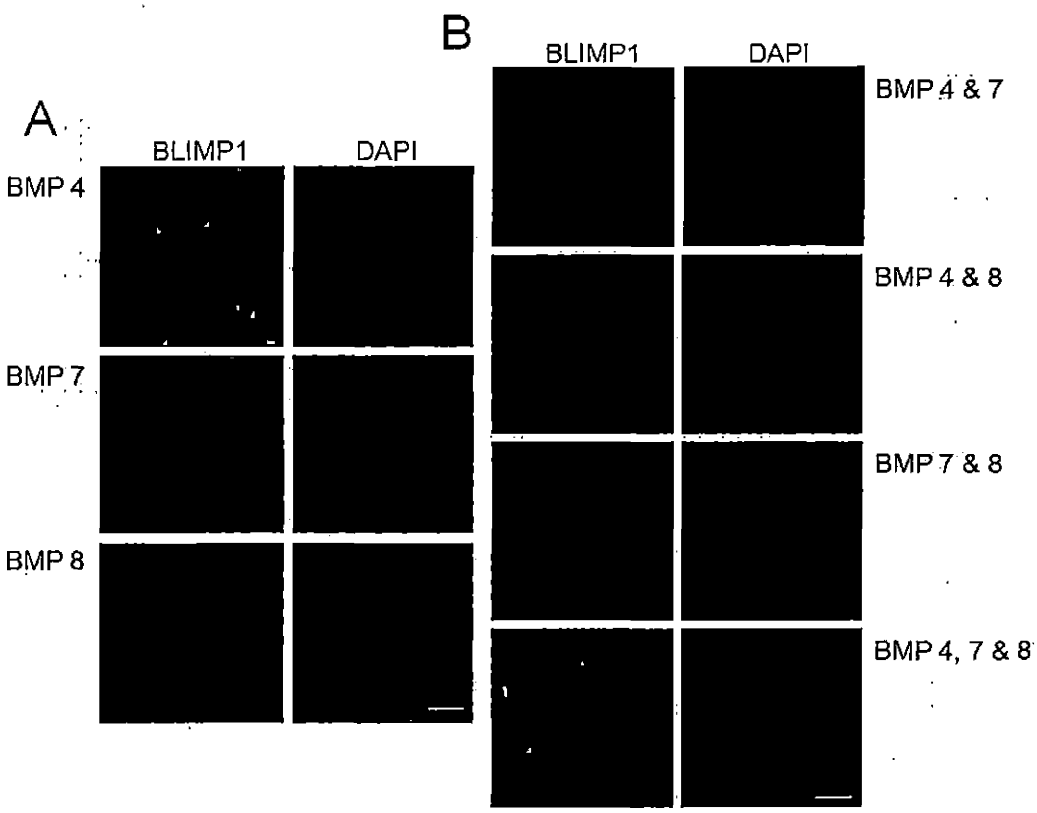

Figure 9. Day Five Immunocytochemistry Analysis of H9 hESC Bone Morphogenetic Protein Treatments. (A) Immunocytochemistry analysis of BMP4, BMP7 and BMP8 treated H9 hESC cultures revealed that BMP4 treatment alone was sufficient to induce BLIMP1 expression. (B) In co-treatment cultures, BLIMP1 expression was restricted to cultures differentiated in BMP4 containing media. BMP7 reduced the effect of BMP4 in the absence of BMP8. Representative images taken at 10X. Scale bar = 50 microns.

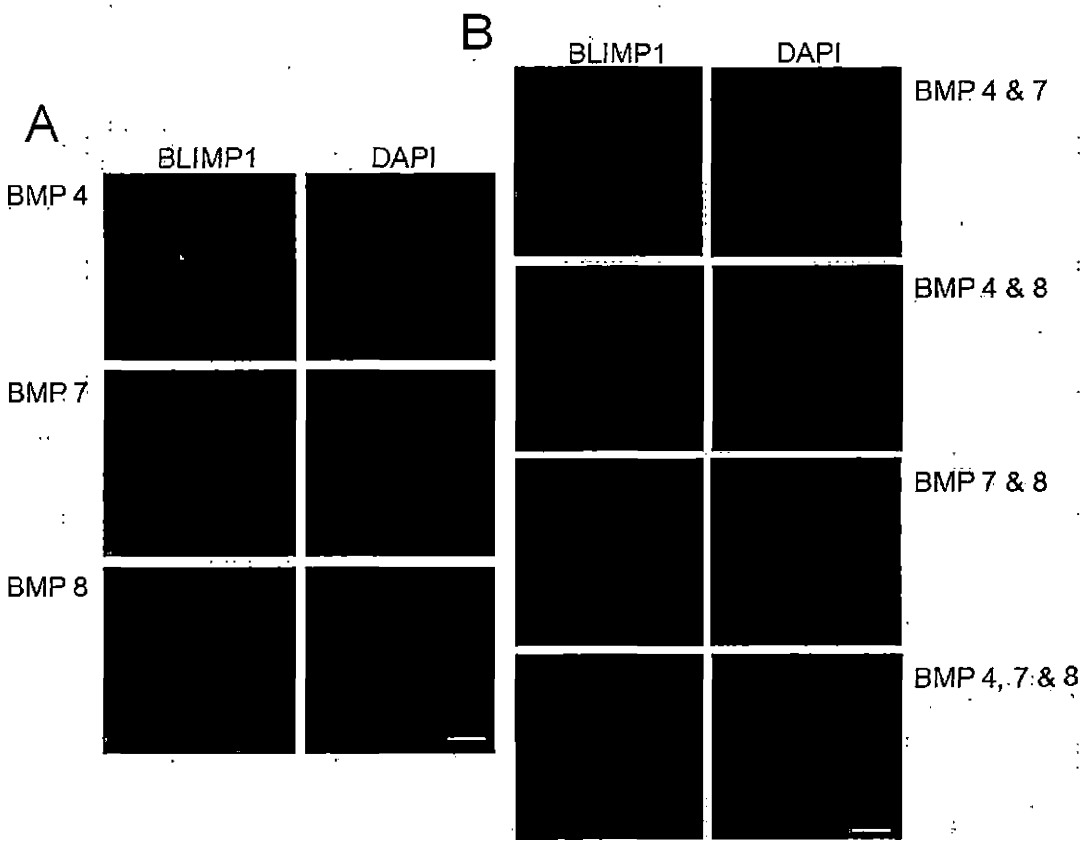

Figure 10. Day Five Immunocytochemistry Analysis of Riv9 hiPSC Bone Morphogenetic Protein Treatments. (A) Immunocytochemistry analysis of BMP4, BMP7 and BMP8-treated Riv9 hiPSC cultures revealed the presence of BLIMP1-immunoreactive cells only when BMP4 was added to the differentiation media. (B) BLIMP1 expression was restricted to BMP4 containing cultures. BMP7 did not diminish the effect of BMP4 to the same extent as H9 hESC. Similarly, to hESC BLIMP1 expression was not detected until day five in Riv9 hiPSC. Representative images taken at 10X. Scale bar = 50 microns.

However, five day BMP-induced BLIMP1 expression was restricted to BMP treatments specifically containing BMP4. This data supports evidence from the mouse model that BMP4 is a prerequisite for BLIMP1 expression and PGC specification.

In order to improve the activation of BLIMP1 expression, addition of BMP4 was increased to two fold. The boost method has been previously used to saturate receptors and achieve higher levels of cascade activation. Comparison of four and five day BMP treatment immunocytochemistry confirmed that increasing the amount of BMP4 drastically increased the BLIMP1 expressing populations in all treatments (Figure 11). Accordingly, the boost method was used in all downstream experiments.

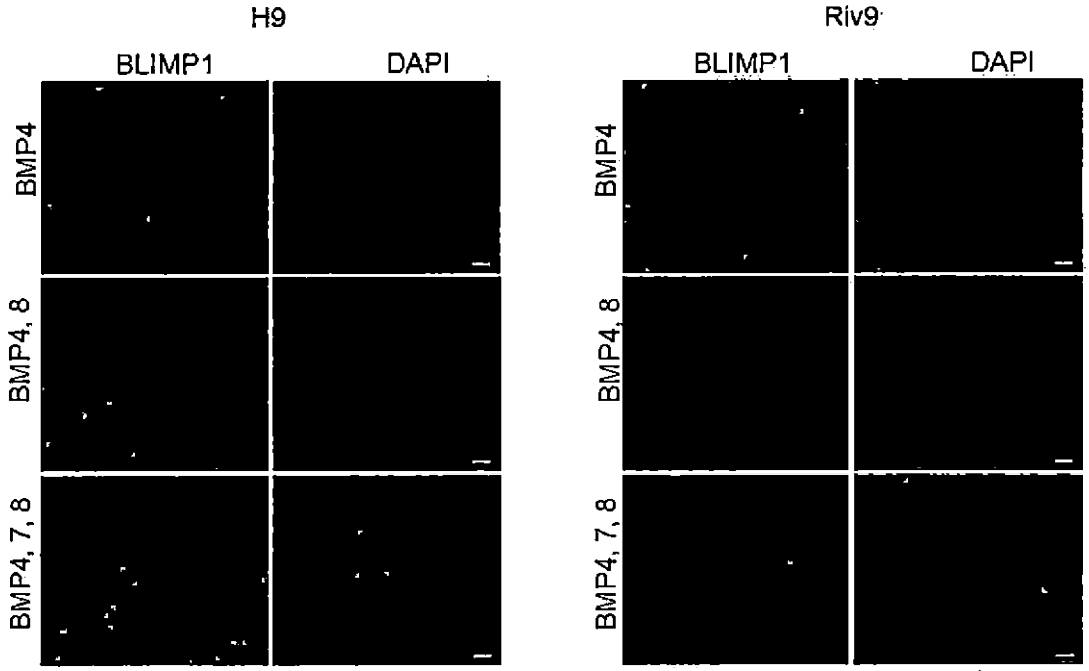

Figure 11. Day Five Immunocytochemistry Analysis of Bone Morphogenetic Protein4 Boost Treatments. Analysis revealed that when the concentration of BMP4 was increased two-fold BLIMP1 induction was increased in both H9 hESC and Riv9 hiPSC. Representative images taken at 10X. Scale bar equals 50 microns.

The proportion of H9 hESC and Riv9 hiPSC that expressed BLIMP1 was quantified to determine the efficiency of PGC specification (Figure 12). Quantification of BLIMP1 expressing H9 cells demonstrated that 5% express BLIMP1 after four days of treatment and the proportion increased to 35% on day five. On the other hand, BLIMP1 expression was only detected in day five culture treatments of Riv9 hiPSC demonstrating a delay in PGC differentiation. However, the percentage of Riv9 cells that expressed BLIMP1 was higher at the onset of protein expression on day five compared to H9; 48% in BMP4

treatments and 39% in BMP4, 7 and 8 treatments. Additionally, we found that BMP4 and co-induction of BMP4, 7 & 8 gave rise to significantly higher percentages of BLIMP1-positive cells in both hESC and hiPSC cultures.

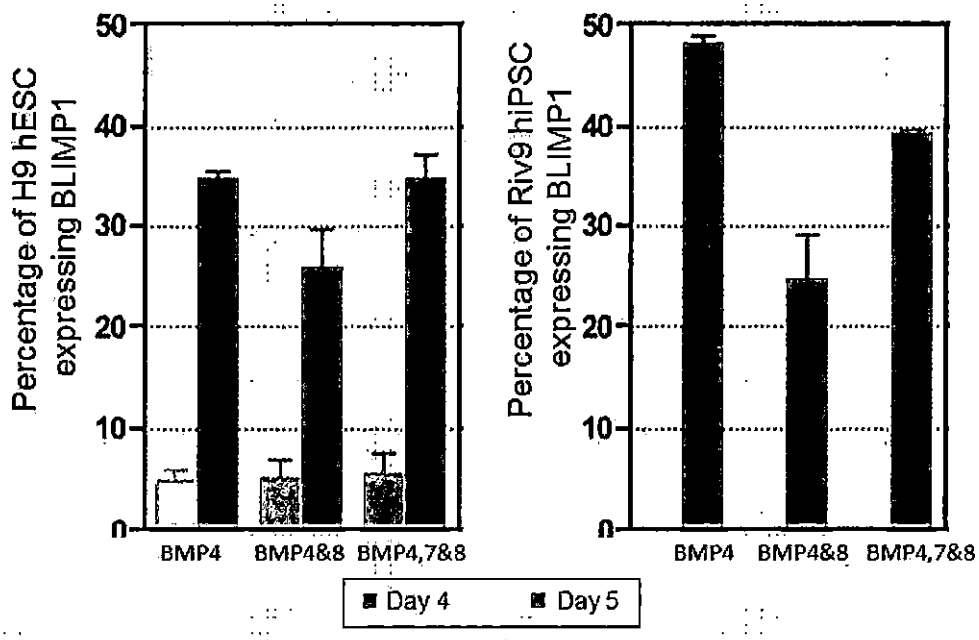

Figure 12. Quantification of B-Lymphocyte Induced Maturation Protein1-Expressing Cells Derived from hESC and hiPSC in the Presence of Different Bone Morphogenetic Proteins. Data were collected by direct scoring for cells showing BLIMP1 staining normalized to the total cell number in a 4X image capture, indicated by DAPI nuclear staining.

The real-time Q-PCR analysis reflected at least a 50% downregulation of OCT4 expression levels on day four, which continued to decrease on day five in both hESC and hiPSC. DAZL and CD117 expression was also reduced in PGC

compared to hESC and hiPSC. As predicted there was a significant upregulation of BLIMP1 following BMP treatment. PGC related transcripts Stella and VASA were also upregulated in PGC compared undifferentiated cells, however expression levels did not differ significantly between day four and day five timepoints. Sox17, an early PGC transcript, was also upregulated in the hESC-derived and hiPSC-derived PGC. (Figure 13 and Figure 14)

Furthermore, to demonstrate the relationship between BMP signaling and the initiation of BLIMP1 expression, BMP receptors were inhibited. Dorsomorphin, a molecular antagonist of BMP receptors, was added to the differentiation media with the BMP treatments. Following five days of differentiation in the presence of BMP treatment and dorsomorphin, expression of BLIMP1 was diminished (Figure 15).

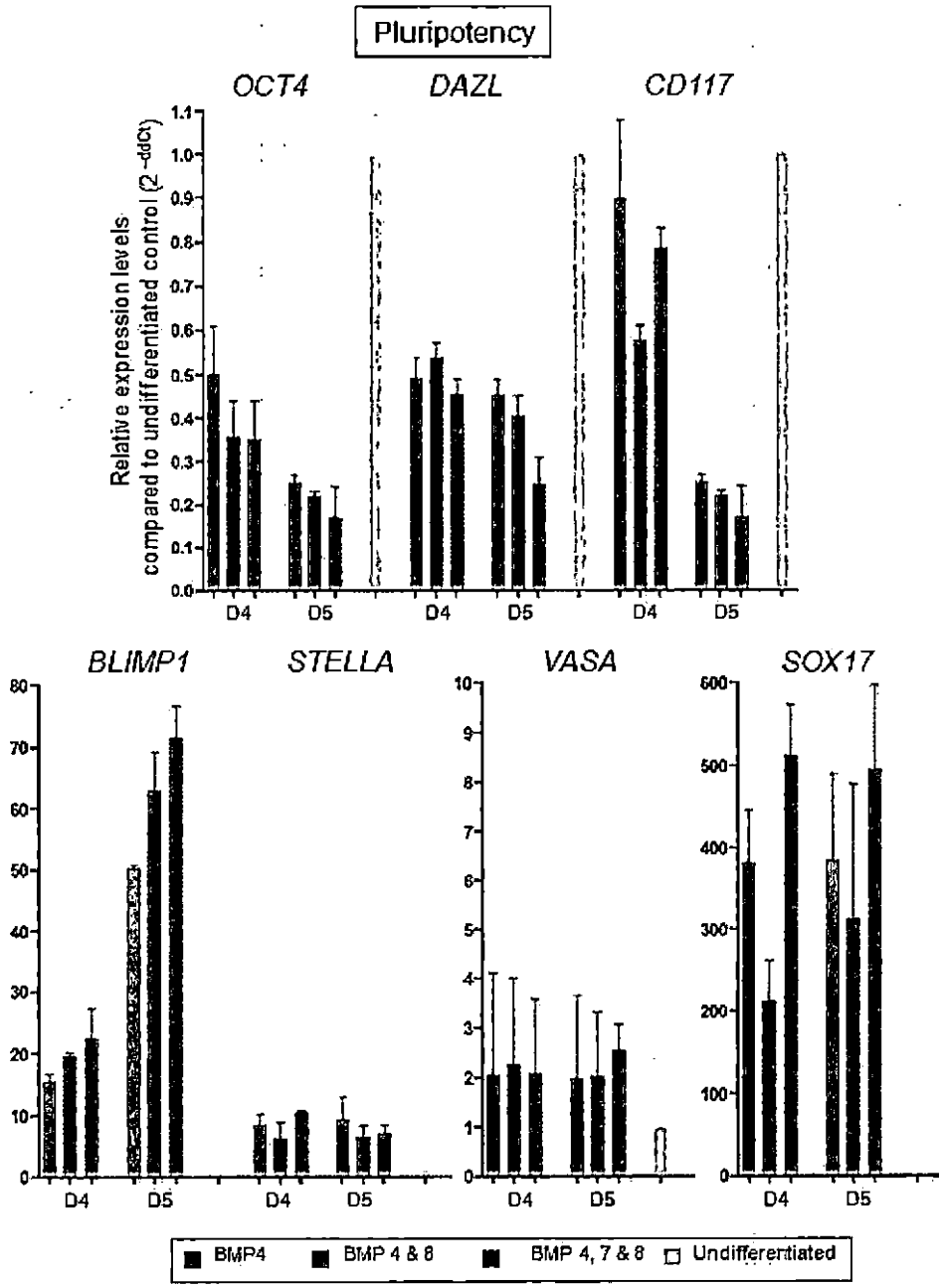

Figure 13. Real-Time Quantitative-Polymerase Chain Reaction Analysis of H9 hESC Following Four and Five Days of Bone Morphogenetic Protein Treatments. Relative transcript expression levels of three pluripotency genes, OCT4, DAZL and CD117. Normalized data presented as mean+SEM.

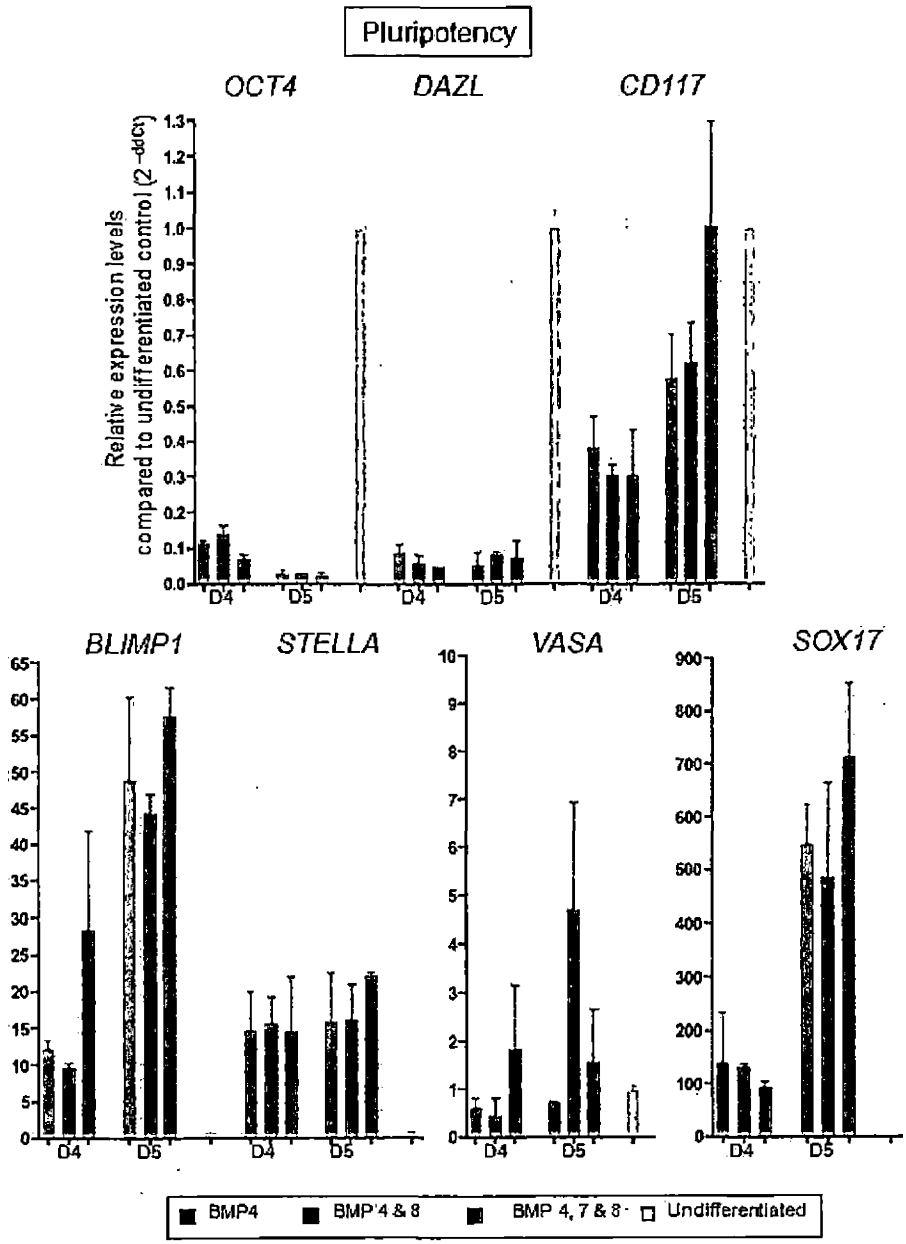

Figure 14. Real-Time Quantitative-Polymerase Chain Reaction Analysis of Riv9 hiPSC Following Four and Five Days of Bone Morphogenetic Protein Treatments. Relative transcript expression levels of three pluripotency genes, OCT4, DAZL and CD117. Normalized data presented as mean+SEM.

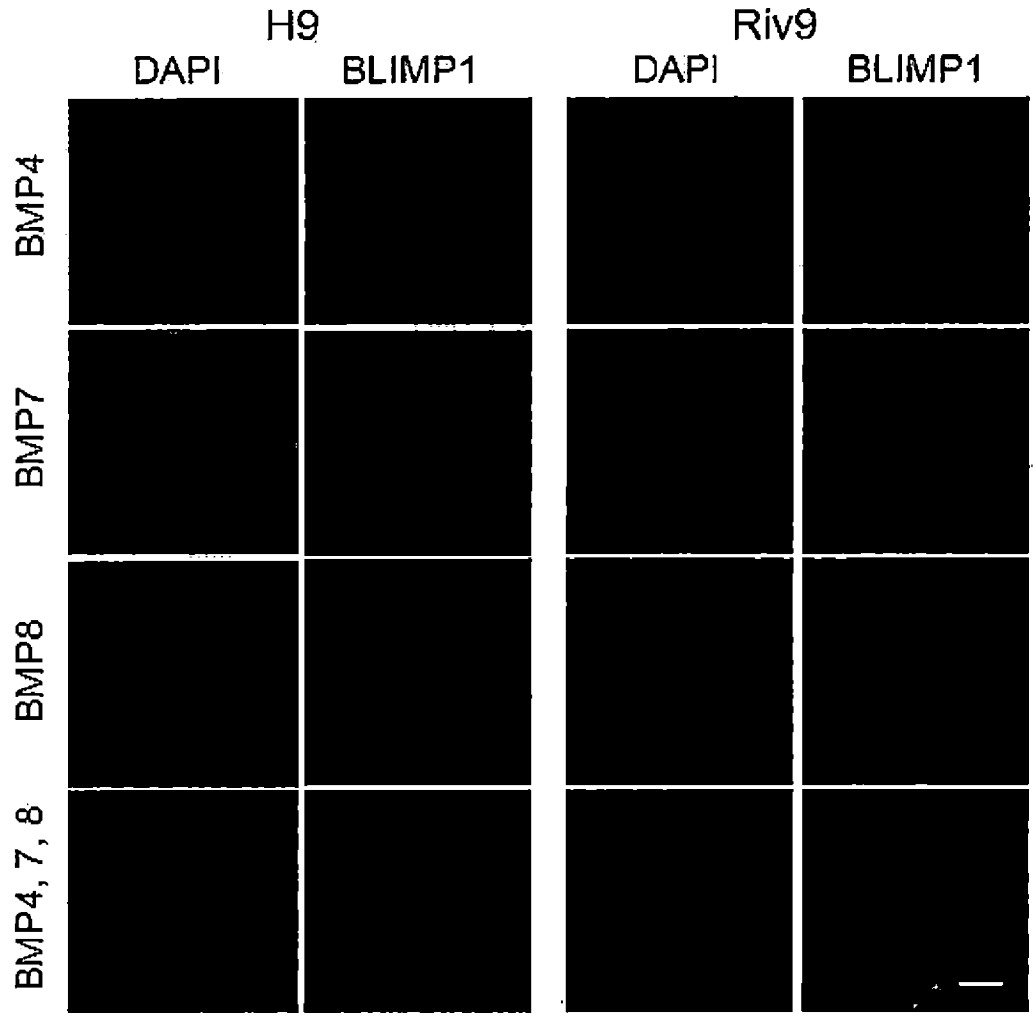

Figure 15. Dorsomorphin Inhibited Bone Morphogenetic Protein Signaling. H9 hESC and Riv 9 hiPSC cultured in the presence of dorsomorphin significantly diminished the expression of BLIMP1. Representative images taken at 10X. Scale bar = 50 microns.

Surface Marker CXCR-4 Isolates PGC From Heterogeneous Populations

Magnetic activated cell sorting (MACS) was performed to characterize cell fractions based on the expression of cell surface proteins. Antibodies previously demonstrated to identify PGC were used to sort cells accordingly. Real-time Q-PCR analysis was used to create a transcription profile of the cell isolated based on the expression of CD117, CXCR-4 and SSEA1 (Figure 16). The expression profiles revealed that CXCR-4 positive hESC and hiPSC cells highly upregulate PGC associated transcripts, SOX17, BLIMP1, NANOG and DAZL. By comparison SSEA1 positive cell sorting only isolated hiPSC-derived PGC, the hESC SSEA1 positive cells did not show upregulation of PGC transcripts. Furthermore, CD117 positive sorting isolated cells expressing somatic transcript, such as HOXB1.

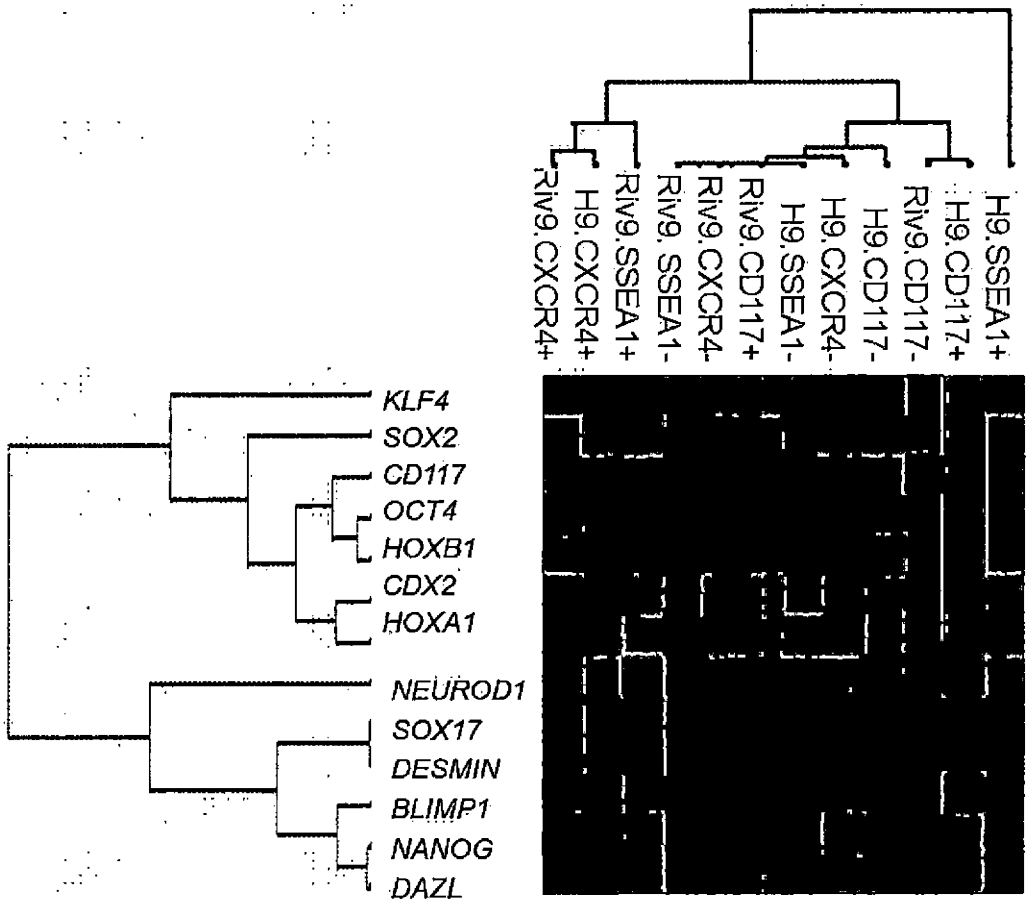

Figure 16. Heat Map of CD117, CXCR4 and SSEA1 Cell Fractions Isolated by Magnetic Activated Cell Sorting. CXCR-4 expressing hESC and iPSC upregulated PGC associated genes BLIMP1, NANOG and DAZL. A similar expression pattern was observed in SSEA1 expressing cells but to a lesser extent. Conversely, CD117 expressing cells upregulated a conflicting set of genes.

B-Lymphocyte Maturation Protein 1a Restricted hESC To Primordial Germ Cell Differentiation

Amino terminus specific primers for BLIMP1a and BLIMP1b were used to determine which variance is responsible for the transcriptional regulation of PGC specification. Cell pellets were collected from four and five day BMP-treated cultures and semi-quantitative PCR was performed to identify BLIMP1 variance. Our data revealed that BLIMP1a was upregulated in all BMP-induced PGC populations whereas BLIMP1b was not detected in any cells. However, another PRDM transcript BLIMP14 was restricted to hESC (Figure 17).

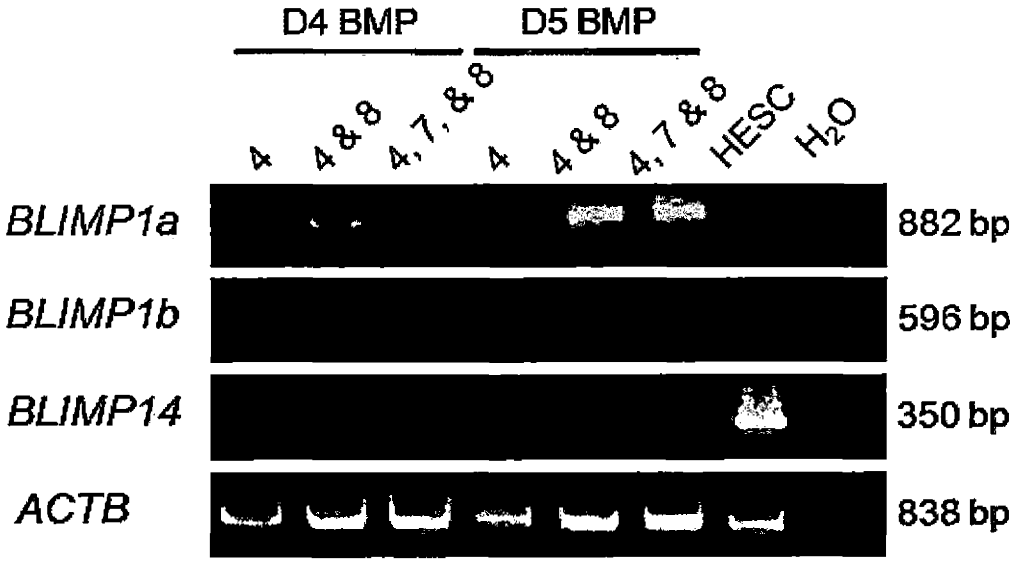

Figure 17. Semi-Quantitative Polymerase Chain Reaction Analysis of B-Lymphocyte Induced Maturation Protein1 Variance Expression. PCR of BMP-treated and undifferentiated hESC cDNAs was performed using BLIMP1a and BLIMP1b specific forward primers. BLIMP14, a proposed upstream gene of BLIMP1, was only expressed in hESC. ACTB was used as a loading control and water as a RT control.

H9 hESC were induced to overexpress either BLIMP1a or BLIMP1b for three days to demonstrate the downstream effects of transcriptional regulation by each variance. To precisely analyze the changes at the cellular level, single cell real-time Q-PCR was performed on BLIMP1a and BLIMP1b overexpressing cells (Figure 18 and Figure 19). Threshold cycle (Ct) values from sets of BLIMP1a, BLIMP1b and uninduced single cells revealed differential amplification of transcripts from individual single cells. In general high background transcript expression levels were observed in the uninduced cells, especially BLIMP1. Statistical analysis revealed higher Ct values for pluripotency markers OCT4 and cMYC in both BLIMP1a and BLIMP1b cells compared to uninduced cells. Concerning the Ct values of OCT4 BLIMP1a maintain expression at a higher level than BLIMP1b. Moreover, STELLA transcripts had significantly lower Ct values in BLIMP1a and BLIMP1b single cells compared to uninduced. Conversely, DAZL Ct values in BLIMP1a cells was significantly higher compared to BLIMP1b and uninduced cells. Notably, HOXB1 a somatic transcript demonstrated lower Ct values in all uninduced single cells, compared to BLIMP1a-induced cells.

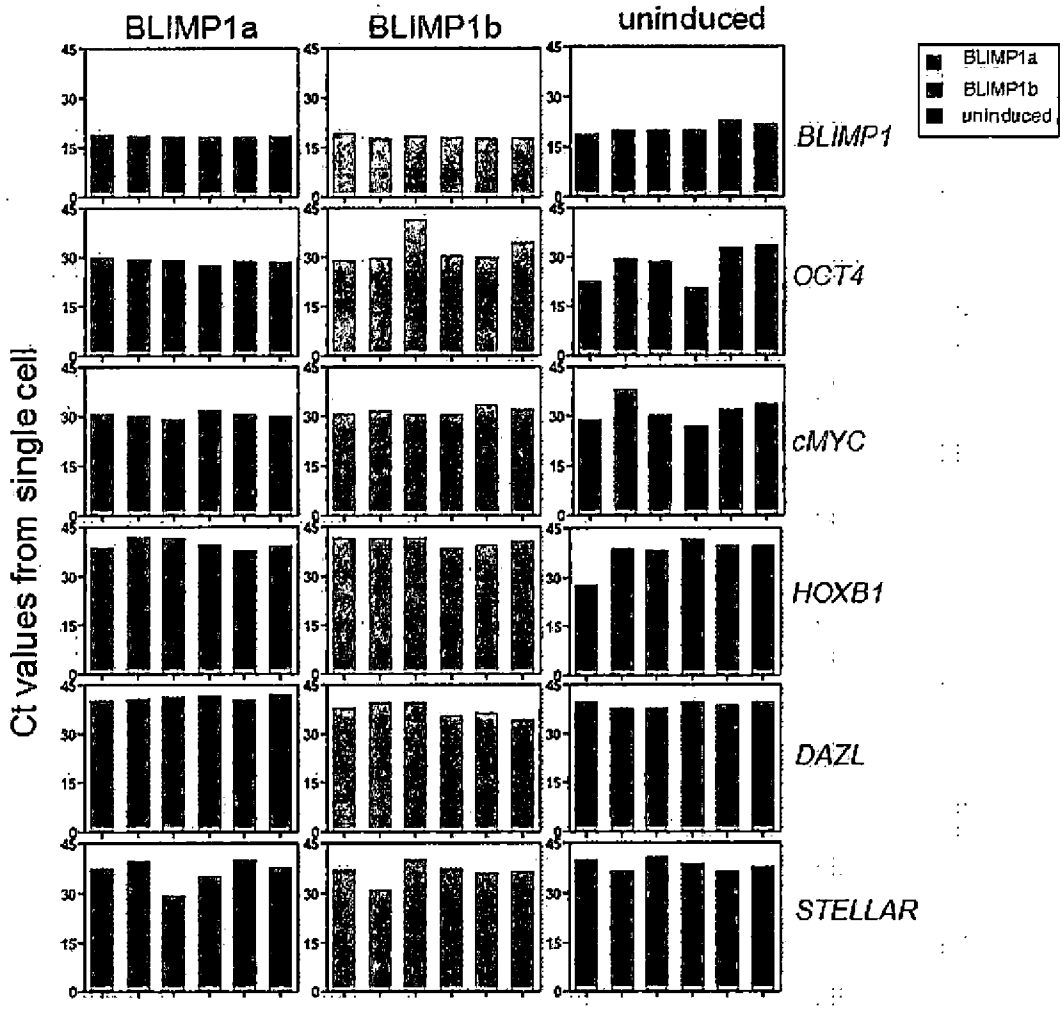

Figure 18. Single Cell Real-Time Quantitative-Polymerase Chain Reaction Analysis Part 1. Single cell real-time Q-PCR analysis of six BLIMP1a- and BLIMP1b-overexpressing cells and six uninduced counterparts. Ct values for BLIMP1, OCT4, cMYC, HOXB1, DAZL, and Stella from six replicate single cells are presented.n=6.

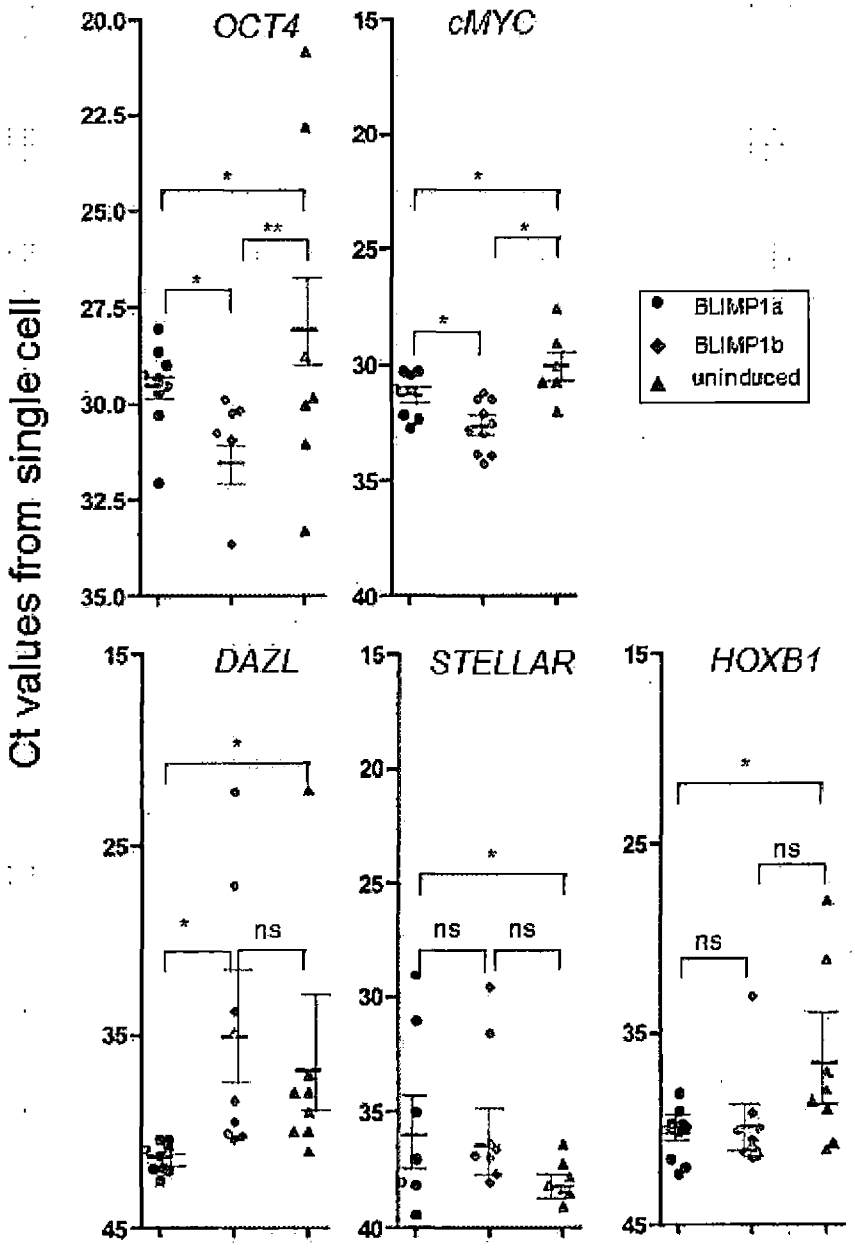

Figure 19. Single Cell Real-Time Quantitative-Polymerase Chain Reaction Analysis Part 2. Statistical data comparing Ct values of BLIMP1, OCT4, DAZL, Stella and HOXB1 from nucleofected BLIMP1a and BLIMP1b overexpressing cells and uninduced counterparts. n=6-10.

Epigenetic Role of B-Lymphocyte Induced Maturation Protein1

The epigenetic status of hiPSC was compared to BMP4 induced PGC using immunocytochemistry for two histone protein methylation patterns, H3K9me2 and H3K27me3. Changes in the histone methylation are correlated with genome-wide DNA demethylation during epigenetic reprogramming of PGC. Based on the mouse model system H3K9me2 levels were predicted to decrease as H3K27me3 levels were predicted to increase. Riv9 hiPSC were used as a baseline for comparison of H3K9me2 and H3K27me3 status. Riv9 hiPSC were determined to express both histone methylation marks (Figure 20).

The relationship between OCT4 expression of pluripotent hiPSC and histone methylation marks was examined by quantifying the intensity levels of co-expression of OCT4 and the histone modifications (Figure 21). High expression levels of OCT4 were observed to be correlated with high levels of H3K9me2 and H3K27me3, correlation coefficient values of 0.591 and 0.554 respectively.

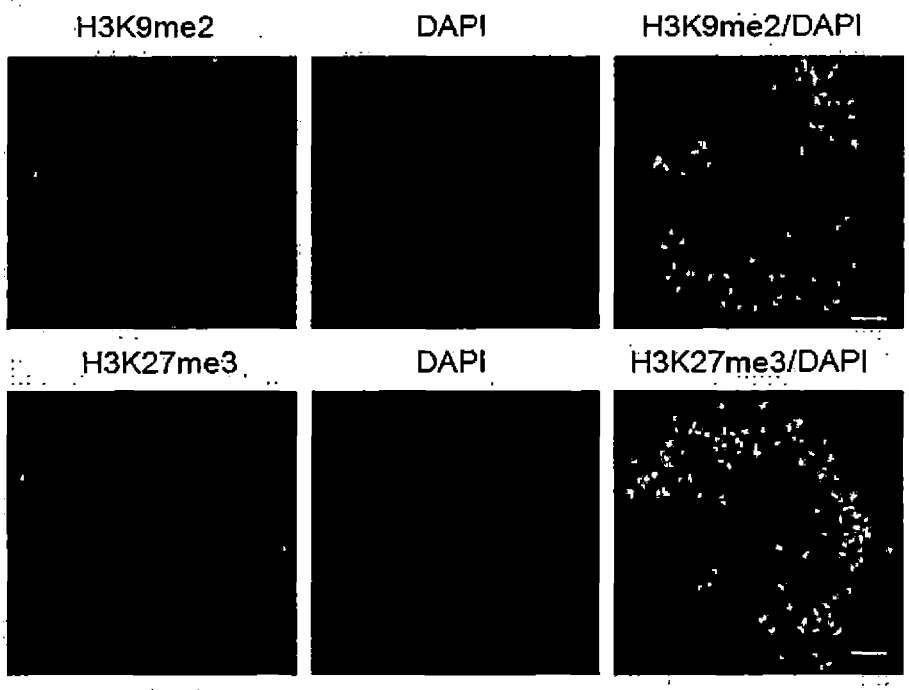

Figure 20. Riv9 hiPSC Histone Methylation Patterns. Riv9 hiPSC displayed ubiquitous expression of H3K9me2 and H3K27me3.

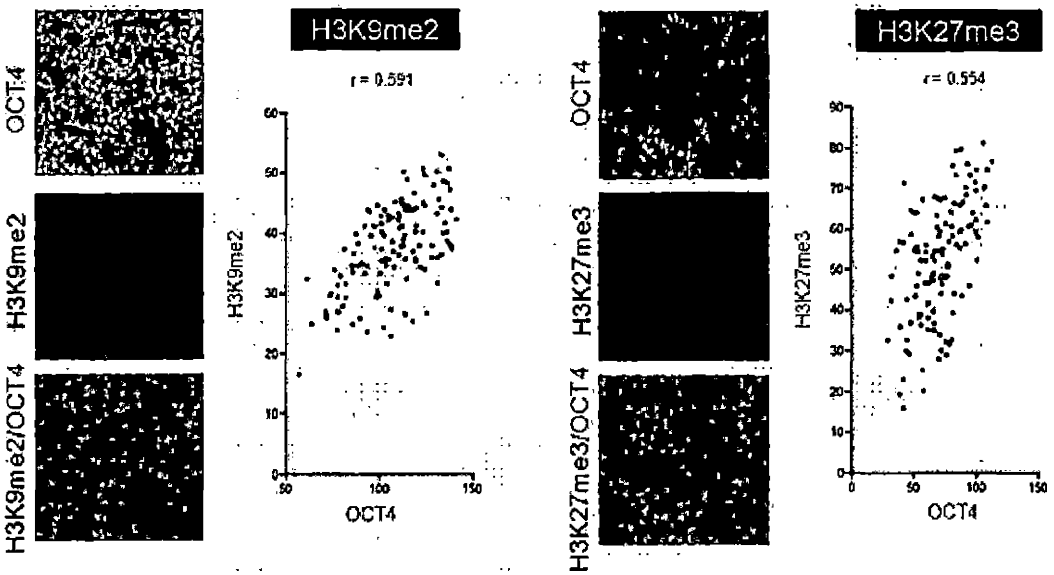

Figure 21. Immunocytochemistry Intensity Analysis of Histone Methylation Patterns and OCT4. Intensity levels of protein expression within 200 individual cells which co-expressed H3K9me2 and OCT4. Cells co-expressing H3K27me3 and OCT4 were quantified using Image J analysis software. Coefficients of correlation were determined, and supported a positive relationship for the histone markers and OCT4. n=200.

When the pluripotent cells were spontaneously differentiated the methylation pattern changed (Figure 22). This data demonstrates that epigenetic profiles change as the pluripotent cells undergo *in vitro* differentiation. Specifically, while pluripotent cells experienced a reduction in the occurrence of H3K9me2, H3K27me3 levels were maintained.

BMP treatments were used to induce the PGC fate so the corresponding epigenetic profile could be determined. As expected H3K9me2 was reduced during PGC specification, however the levels of H3K27me3 were maintained rather than increasing (Figure 23). To further explore the relationship between histone methylation levels and PGC specification the intensity level of BMP-induced hESC was quantified to determine the correlation between H3K27me3 and BLIMP1 (Figure 24). The maintenance of H3K27me3 was shown to be positively correlated with the onset of BLIMP1 expression in PGC.

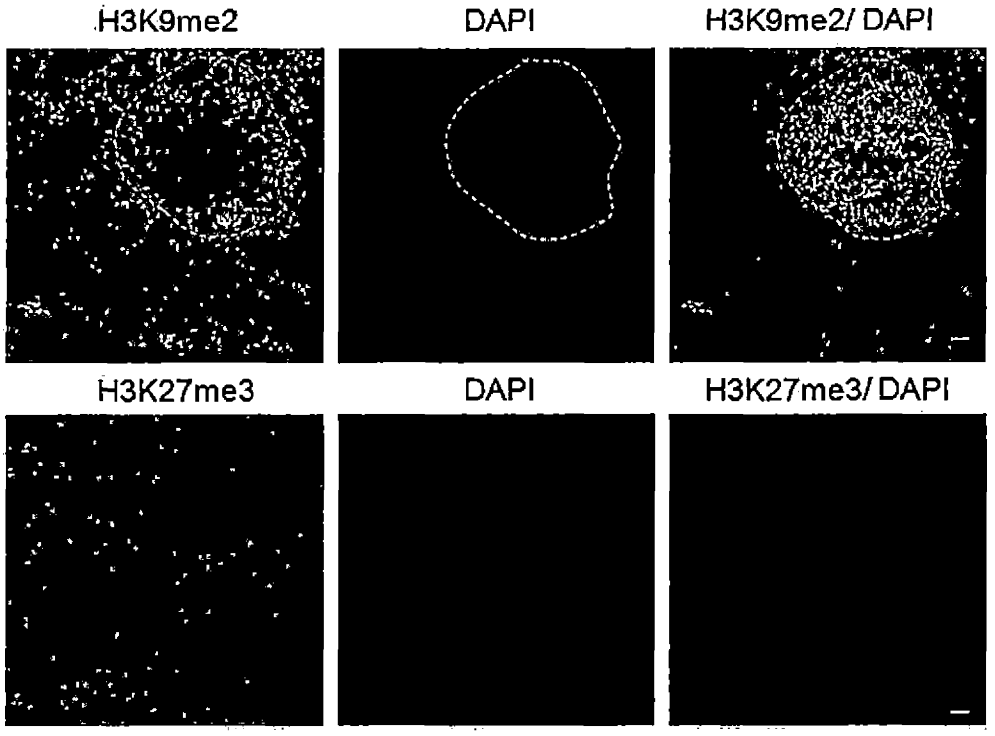

Figure 22. Spontaneously Differentiating Riv9 hiPSC Histone Methylation Patterns. Spontaneous differentiation of Riv9 hiPSC resulted in deviation in the pattern of occurrence of H3K9me2 among the several cell types. Conversely, H3K27me3 levels were maintained. Following five days of differentiation residual undifferentiated regions maintained pluripotent methylation patterns (outlines in white dashes). Images taken at 4X. Scale bar = 50 microns.

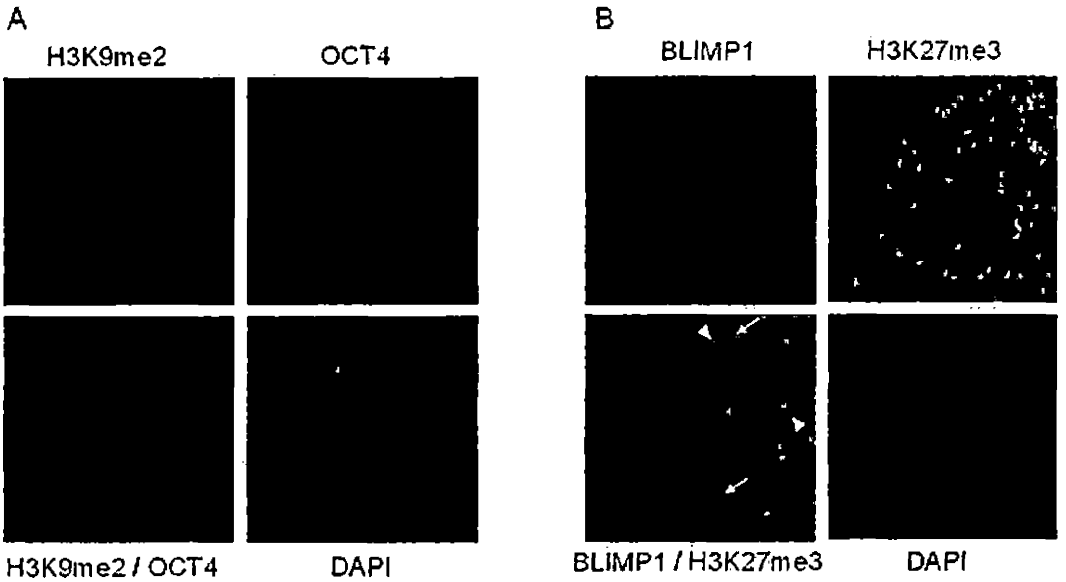

Figure 23. Histone Methylation Patterns of Induced Primordial Germ Cells. (A) Loss of H3K9me2 in PGC induced cultures. As PGC induced cultures differentiated, demonstrated by loss of OCT4, H3K9me2 levels were reduced. (B) Co-expression of H3K27me3 and BLIMP1. BLIMP1 positive cells appeared to express and maintained H3K27me3 expression.

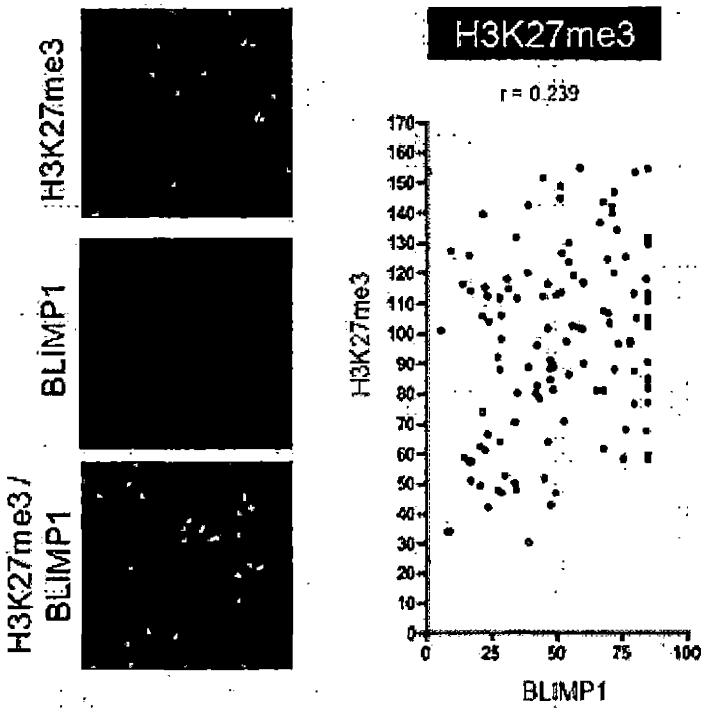

Figure 24. Immunocytochemistry Intensity Analysis of H3K27me3 and B-Lymphocyte Induced Maturation Protein1. BLIMP1 positive cells unequivocally expressed H3K27me2. However, BLIMP1 was weakly correlated with the expression of H3K27me3 epigenetic marks. n=200.

CHAPTER FIVE

DISCUSSION

Optimized Induction and Isolation of Primordial Germ Cells

An *in vitro* time-course was utilized to determine optimal conditions to induce and isolate the founding population of the germline. Derivation of a large population of PGCs will enable wide-scale manipulation of these significant progenitors, and improve current knowledge on the unique processes of germline differentiation. Mouse paradigms have confirmed the significance of BMP4 as an initiating mechanism of the germ cell fate (Lawson et al., 1999). Furthermore, co-induction of mouse models was demonstrated to improve the efficiency of PGC induction (Ohinata et al, 2009). Our results indicate that the role of BMP signaling during the PGC specification is evolutionarily conserved. Specifically, BMP4 is both necessary and sufficient to induction PGC specification as indicated by the onset of BLIMP1 expression in hESC and hiPSC. In the absence of BMP4 signaling *in vitro* PGC specification is not induced. Furthermore, presence of BMP receptor antagonist, dorsomorphin, was sufficient to prevent BLIMP1 activation. Thus, a signaling cascade initiated by BMP4 leads to the activation of germline transcriptional regulator BLIMP1 and initiates PGC specification.

Moreover, the co-induced cultures with BMP4 and 8 exhibited lower induction efficiencies than observed in mouse models. Given the inhibitory role of BMP8 against non-PGC signaling from neighboring somatic niches within the

mouse embryo proper, we speculate that *in vitro* cultures which lack niche organization accordingly do not benefit from BMP8 inhibition. Interestingly the addition of BMP7, required for early PGC proliferation (Ross et al., 2007), added to the effect of BMP4 and 8 to increase the efficiency of PGC specification. Given the miniscule expression of BLIMP1 in BMP4 and 7 treatments it can be assumed that interaction of BMP7 and BMP8 is required to improve the PGC induction. Whether this interaction involves the inhibition of BMP7 by BMP8 to promote induction is yet to be explored. Protein quantification data reflect that the highest efficiency of BLIMP1 expression in H9 hESC was achieved following BMP4, 7 and 8 treatment. Our immunocytochemistry data is supported by real-time Q-PCR data in which the highest relative expression levels were also observed in the BMP4, 7 and 8 treatments. On the other hand, data for Riv9 reflects higher percentages of BLIMP1 expressing cells in BMP4 treatments, whereas the Q-PCR relative expression levels of BMP4 and BMP4, 7, and 8 were not significantly different. The higher percentage of BLIMP1 cells in BMP4 treatment can be related to transcription differences in the individual cells. Thus, BMP4 cells express lower transcription levels of BLIMP1, so that a smaller population of BMP4, 7 and 8 cells were able to achieve similar levels of BLIMP1 expression. Single cell analysis utilizing a BLIMP1 reporter line would clarify these reports, and avoid assumptions caused by bulk culture RNA.

Based on the real-time Q-PCR data BMP signaling result is followed by transcription of BLIMP1 by day four in both hESC and hiPSC cultures. However

immunocytochemistry revealed that although transcripts are present in the day four BMP-treated Riv9 cells, protein expression is delayed until day five. Nevertheless, immunocytochemistry and real-time Q-PCR reflected similar transcript and protein expression levels in five day cultures achieved by the addition of BMP4, 7 and 8. Accordingly, once cells were induced for five days isolation was performed by MACS. MACS is a preferred method of precisely isolating small fractions of stem cells from heterogeneous populations (Palmon et al., 2012). Given the variable propensity of hESC and hiPSC to differentiate into specific lineages, MACS isolation is an ideal tool for isolating PGC. Isolation of germ cells has been previously accomplished by sorting for cell surface markers, CD177, CXCR-4 and SSEA1 (Xiang-long et al., 2005; Geijsen et al., 2004; Knaut et al., 2003; Molyneaux et al., 2003). Genetic profiles of CD117, CXCR-4 and SSEA1 positive and negative cell fractions were analyzed to determine which marker would isolate our cells of interest. CXCR-4 is related to the survival and migration of PGC (Molyneaux et al., 2003) and identified the early PGC population of interest. The CXCR-4 positive cell genetic profile was sufficient to characterize the cells fraction as germ-like. Accordingly, the method of five day BMP4, 7 and 8 co-induction followed by CXCR-4 MACS isolation can be repeatedly utilized to isolate large populations of PGC in order to interrogate mechanisms of germ cell differentiation. Future studies will attempt to clone a BLIMP1 reporter in order to further optimize the identification and modeling of the germline and unique processes like epigenetic erasure and meiosis.

B-Lymphocyte Induced Maturation Protein1a Restricted hESC to Germ Cell Fate

BLIMP1 has been previously identified as the regulator of the germline (Ohinata et al., 2005). As a transcriptional repressor BLIMP1 restricts cells from entering a somatic program and consequently promotes designation to germ cell fate (Kurimoto et al, 2008). Identification of two well described variances of BLIMP1, BLIMP1a and BLIMP1b, has led to debate concerning the variance responsible for germ cell specification. BMP-induced five day cultures differentiating to PGC were examined for the expression of BLIMP1a and BLIMP1b. Transcripts for BLIMP1a were confirmed in every PGC induced culture. Conversely, there was no detection of BLIMP1b in any of the BMP-induced PGC cultures. The data clearly demonstrates that BLIMP1a is responsible for transcriptional repression of the somatic program and PGC specification. Given the disruption of the PR domain exons in BLIMP1b (Gyory et al., 2004), it follows that the protein domain is crucial for functionality of BLIMP1a at the onset of germ cell differentiation.

Single cell analysis reinforced the functional role of BLIMP1a in PGC specification. BLIMP1a expression examined at the cellular level demonstrated expected transcriptional characteristics of PGC. Compared to uninduced counterparts BLIMP1a cells downregulated pluripotency markers as PGC differentiation initiated, whereas STELLA an early marker of PGC (Payer et al., 2006) was upregulated in BLIMP1a cells. Furthermore, BLIMP1a repressed transcription of somatic program marker HOXB1 at the single cell level.

Significant differences in between BLIMP1a and BLIMP1b single cells involved pluripotency-related transcripts, OCT4 and cMYC. Since BLIMP1b expression resulted in downregulation of pluripotency genes, which must be maintained during germline differentiation, it can be assumed that BLIMP1b is functionally inappropriate for germline transcriptional regulation. OCT4 is known to be a crucial to maintaining pluripotency in both hESC and the germline (Pesce et al., 1998; Adjaye et al., 1999; Goto et al., 1999). Specifically in the germline, maintenance of OCT4 has been associated with germ cell survival (Kehler et al., 2004). The data demonstrates a significant distinction in the level of downregulation of OCT4 between BLIMP1a and BLIMP1b as well as a second pluripotency marker cMYC. Consequently, BLIMP1b does not sufficiently maintain the expression of these critical pluripotency genes and is an inappropriate initiator of PGC specification. Alternatively, BLIMP1b may exert its effects to induce human pluripotent stem cells to differentiate into non-germ cell lineages.

Histone Methylation Patterns Were Evolutionarily Conserved

Routine zygotic fusion by haploid gametes necessitates reestablishment of a totipotent identity. Achieving totipotency requires expression of pluripotent transcripts and epigenetic erasure (Surani et al., 2007). *In vivo* mouse modeling has established a pattern of epigenetic reprogramming of the germline.

Immediately following PGC induction repressive methylation patterns responsible for cell type specific gene expression are reduced. Specifically, as DNA is demethylated there is a concomitant loss of H3K9me3. Following demethylation, H3K9me2 euchromatic regions upregulate another repressive modification H3K27me3. H3K27me3 has also been observed in the pluripotent ICM and inactivated X-chromosomes. However, H3K27 is significantly more permissive and thus a more appropriate modification for reestablishing totipotency. (Seki et al., 2004).

These histone methylation marks were examined during early human PGC differentiation to evaluate the evolutionary conformity of epigenetic reprogramming. Prior to comparing germ cell epigenetics across species, the histone methylation pattern of the pluripotent cells was established. The hiPSC, like pluripotent ICM, ubiquitously expressed H3K27me3. H3K9me2 was also expressed in hiPSC, which conflicts with expression of histone 3 lysine 9 trimethylation patterns observed in hESC (Mattout and Meshorer, 2010). Nevertheless, these findings bolster augments that purport the designation of hiPSC as a distinct pluripotent cell type given their source and unique epigenome (Kim et al., 2010; Chin et al., 2009).

Following the onset of BLIMP1 expression in PGC induced cultures rapid and unequivocal loss of H3K9me2 was confirmed. This result was distinct from H3K9me2 patterns in spontaneously differentiating cultures, in which occurrence of several distinct lineage gene expression patterns resulted in heterogeneous

levels of the histone modification. Regarding H3K27me3, wide-spread expression of the histone modification was observed in both hiPSC, spontaneously differentiating and PGC induced cultures. While spontaneously differentiating cell expression of H3K27me3 can be attributed to X-chromosome inactivation (Seki et al., 2004), further examination of PGC expression of H3K27me3 was required. Analysis of the expression intensities of BLIMP1 and H3K27me3, which exhibited a correlation coefficient of 0.239, were not as significant as the mouse model would suggest. One explanation for the weak correlation could result from differences in the H3K27me3 pattern of pluripotent precursors of the germline in mice. Also, given the wide-spread expression of H3K27me3 and the rapid differentiation of PGC *in vitro,* examination of earlier timepoints would have been informative. Observation of histone methylation at timepoints demonstrating the loss of H3K9me3 and subsequent expression of H3K27me3 would be ideal. Capturing these timepoints would clarify the initial expression levels H3K27me3, so that the extent to which the histone modification is fully upregulated could be determined. Regardless, our data suggests correlation at the cellular level between the onset of BLIMP1 and H3K27me3 levels which support epigenetic patterns in the mouse model and confirms the evolutionary conservation of germline epigenetic reprogramming. To our knowledge the correlation of BLIMP1 and H3K27me3 levels is the first indication of an epigenetic role for BLIMP1.

REFERENCES CITED

Adjaye J, Bolton V, Monk M. 1999. Developmental expression of specific genes detected in high-quality cDNA libraries from single human preimplantation embryos. Gene 237:373–383.

Aw TJ, Haas SJ,. Liew D, Krum H. 2005. Meta-analysis of cyclooxygenase-2 inhibitors and their effects on blood pressure. Archives of Internal Medicine 165:490–496.

Blelloch R, Venere M, Yen J, Ramalho-Santos M. 2007. Generation of induced pluripotent stem cells in the absence of drug selection. Cell Stem Cell 1(3):245–247.

Brzezinski JA, Lamba DA, Reh TA. 2010. Blimp1 controls photoreceptor versus bipolar cell fate choice during retinal development. Development 137:619-629.

Chadwick K, Wang L, Li L, Menendez P, Murdoch B, Rouleau A, Bhatia M. 2003. Cytokines and BMP-4 promote hematopoietic differentiation of human embryonic stem cells. Blood 102(3):906-915.

Chatterjee P, Ching Y, Liew CG. 2011. Transfecting and nucleofecting human induced pluripotent stem cells. JOVE 56.

Cheng H, Jiang W, Phillips FM, Haydon RC, Peng Y, Zhou L, Luu HH, An N, Breyer B, Vanichakarn, et al. 2003. Osteogenic activity of the fourteen types of human bone morphogenetic proteins (BMPs). The Journal of Bone & Joint Surgery 85:1544-1552.

Chin MH, Mason MJ, Xie W, Volinia S, Singer M, Peterson C, Ambartsumyan G, Aimiuwu O, Ritchter L, Zhang J. 2009. Induced pluripotent stem cells and embryonic stem cells are distinguished by gene expression signatures. Cell Stem Cell 5(1):111–123.

Dahéron SL, Zaehres H, Lensch W M, Andrews PW, Itskovitz-Eldor J, Daley GQ. 2004. LIF/STAT3 Signaling fails to maintain self-renewal of human embryonic stem cells. Stem Cells 22:770–778

De Sousa Lopes SM, Roelen BA, Monteiro RM, Emmens R, Lin HY, Lawson KA, Mummery CL. 2004. BMP signaling mediated by ALK2 in the visceral endoderm is necessary for the generation of primordial germ cells in the mouse embryo. Genes and Development 18:1838–1849.

Dudley B, Palumbo C, Nalepka J, Molyneaux K. 2010. BMP signaling controls formation of a primordial germ cell niche within the early genital ridges. Developmental Biology 343:84-93.

Eddy EM, Clark JM, Gong D, Fenderson BA. 1981. Origin and migration of primordial germ cells in mammals. Gamete Research 4(4): 333–362.

Egger G, Liang G, Aparicio A, Jones PA. 2004. Epigenetics in human disease and prospects for epigenetic therapy. Nature 429(6990):457–463.

Eguizabal C, Montserrat N, Vassena R, Barragan M, Garreta E, Garcia-Quevedo L, Vidal F, Giorgetti A, Veiga A, Izpisu Belmonte JC. 2011. Complete meiosis from human induced pluripotent stem cells. Stem Cells 29(8):1186–1195.

Extavour CG, Akam M. 2003. Mechanisms of germ cell specification across the metazoans: epigenesis and preformation. Development 130:5869–5884.

Fuchs E, Segre J. 2000. Stem cells: a new lease on life. Cell 100:143-155.

Gehrig SM, van der Poel C, Sayer TA, Schertzer JD, Henstridge DC, Church JE, Lamon S, Russel AP, Davies KE, Febbraio MA, et al. 2012. Hsp72 preserves muscle function and slows progression of severe muscular dystrophy. Nature 484:384-389

Geijsen N, Horoschak M, Kim K, Gribnau J, Eggan K., Daley GQ. 2004. Derivation of embryonic germ cells and male gametes from embryonic stem cells. Nature 427(6970):148–154.

Gerrard L, Rodgers L, Cui W. 2005. Differentiation of human embryonic stem cells to neural lineages in adherent culture by blocking bone morphogenetic protein signaling. Stem Cells 23(9):1234-1241.

Ginsburg M, Snow MH, McLaren A. 1990. Primordial germ cells in the mouse embryo during gastrulation. (1990) Development 110:521-528.

Goldman D, Bailey AS, Pfaffle DL, Masri AA, Christian JL, Fleming WH. 2009. BMP4 regulates the hematopoietic stem cell niche. Blood 114(20):4393-4401.

Goto T, Adjaye J, Rodeck CH, Monk M. 1999. Identification of genes expressed in human primordial germ cells at the time of entry of the female germ line into meiosis. Molecular Human Reproduction 5:851–860.

Gyory I, Fejer G, Ghosh N, Seto E, Wright KL. 2003. Identification of a functionally impaired positive regulatory domain I binding factor 1 transcription repressor in myeloma cell lines. Journal of Immunology 170:3125-3133.

Hao J, Daleo MA, Murphy CK, Yu PB, Ho JN, Hu J, Peterson RT, Hatzopoulos AK, Hong CC. 2008 Dorsomorphin, a selective small molecule inhibitor of BMP signaling, promotes cardiomyogenesis in embryonic stem cells. PLoS ONE 3(8):e2904.

Hay DC, Sutherland L., Clark J, Burdon T. 2004. Oct-4 knockdown induces similar patterns of endoderm and trophoblast differentiation markers in human and mouse embryonic stem cells. Stem Cells 22(2):225–235.

Henderson J.K, Draper JS, Baillie HS, Fishel S, Thomson JA, Moore H, Andrews PW. 2002. Preimplantation human embryos and embryonic stem

cells show comparable expression of stage-specific embryonic antigens. Stem Cells 20(4):329–337.

Hübner K, Fuhrmann G, Christenson LK, Kehler J, Reinbold R, De La Fuente R, Wood J, Strauss III JF Boiani M, Scholer HR. 2003. Derivation of oocytes from mouse embryonic stem cells. Science 300(5623):1251-1256.

Hull MG, Glazener CM, Kelly NJ, Conway DI, Foster PA, Hinton RA, Coulson C, Lambert PA, Watt EM, Desai KM. 1985. Population study of causes, treatment, and outcome of infertility. BMJ 291(6510):1693–1697.

Itman C, Mendis S, Barakat B, Loveland KL. 2006. All in the family: TGF-β family action in testis development. Reproduction 132:233-246.

Johnson AD, Crother B, White ME, Patient R, Bachvarova RF, Drum M, Masi T. 2003. Regulative germ cell specification in axolotl embryos: A primitive trait conserved in the mammalian lineage. Philosophical Transaction of the Royal Society B Biological Science 358:1371-9.

Kathiresan S, Voight BF, Purcell S, Musunuru K, Ardissino D, Mannucci PM, Anand S, Engert JC, Samani NJ, Schunkert H, et al. 2009. Genome-wide association of early-onset myocardial infarction with single nucleotide polymorphisms and copy number variants. Nature Genetics 41(3):334–341.

Kehler J, Tolkunova E, Koschorz B, Pesce M, Gentile L, Boiani M, Lomeli H., Nagy A, McLaughlin KJ, Scholer HR. 2004. Oct4 is required for primordial germ cell survival. EMBO Reports 5(11):1078–1083.

Kim D, Kim CH, Moon J, Chung YG, Chang MY, Han BS, Ko S, Yang E, Cha K, Lanza R, et al. 2009. Generation of human induced pluripotent stem cells by direct delivery of reprogramming proteins. Cell Stem Cell 4(6):472-476.

Kim K, Doi A, Wen B, Ng K, Zhao R, Cahan P, Kim J, Aryee MJ, Ji H, Ehlich LIR, et al. 2010. Epigenetic memory in induced pluripotent stem cells. Nature. 467(7313):285–290.

Knaut H, Werz C, Geisler R. The Tubingen 2000 Screen Consortium, Nusslein-Volhard C. 2003. A zebrafish homologue of the chemokine receptor Cxcr4 is a germ-cell guidance receptor. Nature 421(6920):279–282.

Kurimoto K, Yabuta Y, Ohinata Y, Shigeta M, Yamanaka K, Saitou M. 2008. Complex genome-wide transcription dynamics orchestrated by Blimp1 for the specification of the germ cell lineage in mice. Genes & Development 22:1617-1635.

Lanza R. 2009. Essential of stem cell biology. 2nd ed. Academic Press: total pages

Lawson K, Dunn N, Roelen B, Zeinstra L, Davis A, Wright C, Korving J, Hogan B. 1999. BMP4 is required for the generation of primordial germ cells in the mouse embryo. Genes & Development 13:424-436

Lawson KA, Hage WJ. (2007). Clonal analysis of the origin of primordial germ cells in the mouse. Chichester (UK): John Wiley & Sons, Ltd. Ciba Foundation Symposium 182 - Germline Development 68–91.

Marques-Mari AI, Lacham-Kaplan O, Medrano JV, Pellicer A, Simón C. 2009. Differentiation of germ cells and gametes from stem cells. Human Reproduction Update 15(3):379-390.

Mattout A, Meshorer E. 2010. Chromatin plasticity and genome organization in pluripotent embryonic stem cells. Current Opinion in Cell Biology 22(3):334–341.

Mitalipov S, Wolf D. 2009. Totipotency, pluripotency and nuclear reprogramming. Advances Biochemical Engineering/Biotechnology 114:185-199

Molyneaux, K. A., Zinszner, H., Kunwar, P. S., Schaible, K., Stebler, J., Sunshine, M. J., O'Brien, W., et al. (2003). The chemokine SDF1/CXCL12 and its receptor CXCR4 regulate mouse germ cell migration and survival. Development 130(18)4279–4286.

Ohinata Y, Ohta H, Shigeta M, Yamanaka K, Wakayama T, Saitou M. 2009. A signaling principle for the specification of the germ cell lineage in mice. Cell 137: 571-584

Ohinata Y, Payer B, O'Carroll D, Ancelin K, Ono Y, Sano M, Barton SC, Obukhanych T, Nussenzweig M, Tarakhovsky A, et al. 2005. Blimp1 is a critical determinant of the germ cell lineage in mice. Nature 436:207-213

Palmon A, David R, Neumann Y, Stiubea-Cohen R, Krief G, Aframian DJ. 2012. High-efficiency immunomagnetic isolation of solid tissue-originated integrin-expressing adult stem cells. Methods 56(2):305-309.

Payer B, Chuva de Sousa Lopes S. M, Barton SC, Lee C, Saitou M, Surani MA. 2006. Generation of stella-GFP transgenic mice: a novel tool to study germ cell development. Genesis 44(2):75–83.

Pesce M, Gross MK, Scholer HR. 1998. In line with our ancestors: OCT-4 and the mammalian germ. Bioessays 20:722–732.

Ross A, Munger S, Capel B. 2007. Bmp7 regulates germ cell proliferation in mouse fetal gonads. Sexual Development 1(2):127–137.

Sabour D, Arauzo-Bravo MJ, Hubner K, Ko K, Greber B, Gentile L, Stehline M, Scholer HS. 2011. Identification of genes specific to mouse primordial germ cells through dynamic global gene expression. Human Molecular Genetics 20:115-125.

Saitou M, Yamaji M. 2010. Germ cell specification in mice: signaling, transcription regulation, and epigenetic consequences. Reproduction 139(6):931-942.

Sasaki N, Hirano T, Kobayashi K, Toyoda M, Miyakawa Y, Okita H, Kiyokawa N, Akutsu U, Nishihara S. 2010. Chemical inhibition of sulfation accelerates neural differentiation of mouse embryonic stem cells and human induced pluripotent stem cells. Biochemical and Biophysical Research Communications 401(3):480–486.

Seki Y, Hayashi K, Itoh K, Mizugaki M, Saitou M, Matsui Y . 2005. Extensive and orderly reprogramming of genome-wide chromatin modifications associated with specification and early development of germ cells in mice. Developmental Biology 278:440-458.

Seki Y, Yamaji M, Yabuta Y, Sano M, Shigeta M, Matsui Y, Saga Y, Tachibana M, Shinkai Y, Saitou M. 2007. Cellular dynamics associated with the genome-wide epigenetic reprogramming in migrating primordial germ cells in mice. Development 134:2627–2638.

Shamblott M, Axelmann J, Wang S, Bugg E, Littlefield J, Donovan P, Blumenthal P, Huggins G, Gearhart J. 1998. Derivation of pluripotent stem cells from cultured human primordial germ cells. PNAS 95(23):13726-13731.

Shi Y, Desponts C, Do JT, Hahm HS, Schöler HR, Ding S. 2008. Induction of pluripotent stem cells from mouse embryonic fibroblasts by Oct4 and Klf4 with small-molecule compounds. Cell Stem Cell 3(5):568–574.

Soldner F, Hockemeyer D, Beard C, Gao Q, Bell GW, Cook EG, Hargus G, et al. (2009). Parkinson's disease patient-derived induced pluripotent stem cells free of viral reprogramming factors. Cell 136(5):964-977.

Tam P, Snow M. 1981. Proliferation and migration of primordial germ cells during compensatory growth in mouse embryos. Journal of Embryology 64:133-147.

Takahashi K, Yamanaka S. 2006. Induction of pluripotent stem cells from mouse embryonic and adult fibroblast cultures by defined factors. Cell 126(4):663–676.

Takahashi K, Tanabe K, Ohnuki M, Narita M, Ichisaka T, Tomoda K, Yamanaka S. 2007. Induction of pluripotent stem cells from adult human fibroblasts by defined factors. Cell 131(5):861-872.

Tesar PJ, Chenoweth JG, Brook FA, Davies TJ, Evans EP, Mack DL, Gardner RL, McKay R. 2007. New cell lines from mouse epiblast share defining features with human embryonic stem cells. Nature 448(7150):196-199.

Thomson JA, Itskovitz-Eldor J, Shapiro SS, Waknitz MA, Swiergiel JJ, Marshall VS, Jones JM. 1998a. Embryonic stem cell lines derived from human blastocysts. Science 282(5391):1145-1147.

Thompson JA, Kalishman J, Golos TG, Durning M, Harris CP, Becker RA, Hearn JP. 1995. Isolation of a primate embryonic stem cell line. PNAS 92(17):7844-7848

Thomson JA, Marshall VS. 1998b. Primate embryonic stem cells. Current Topics in Development Biology 38:133-65.

Toyooka Y, Tsunekawa N, Akasu R, Noce T. 2003. Embryonic stem cells can form germ cells in vitro. PNAS 100(20):11457-11462.

Vincent S, Dunn NR, Sciammas R, Shapiro-Shalef M, Davis MM, Calame K, Bikoff EK, Robertson EJ. 2005. The zinc finger transcriptional repressor Blimp1/Prdm1 is dispensable for early axis formation but is required for specification of primordial germ cells in the mouse. Development 132:1315-1325.

Wang P, Rodriguez RT, Wang J, Ghodasara A, Kim SK. 2011. Targeting SOX17 in Human Embryonic Stem Cells Creates Unique Strategies for

Isolating and Analyzing Developing Endoderm. Cell Stem Cell 8(3):335–346.

Weismann, A. 1885. *Die Continuität des Keimplasmas als Grundlage einer Theorie der Vererbung*, Jena: Fischer-Verlag.

Weissman IL, Anderson DJ, Gage F. 2001. Stem and progenitor cells: origins, phenotypes, lineage commitments, and transdifferentiations. Annual Review of Cell Developmental Biology 17:387-403.

Wylie C. 2000. Germ cells. Current Opinion in Genetics & Development 10(4):410–413.

Xiang-long J, Li-qing F, Wen-bin Z, Ya-rong Z, Guang-xiu L. 2005. Research on expression of CD117 on germ cells in human semen. China Journal of Modern Medicine 12.

Xu H, Yi BA, Wu H, Bock C, Gu H, Lui KO, Park JH, Shao Y, Riley AK, Domian IJ, et al. 2012. Highly efficient derivation of ventricular cardiomyocytes from induced pluripotent stem cells with a distinct epigenetic signature. Cell Research 22(1):142–154.

Xu RH, Peck R, Li DS, Feng X, Ludwig T, Thompson J. 2005. Basic FGF and suppression of BMP signaling sustain undifferentiated proliferation of human ES cells. Nature Methods 2:185-190

Yamaji M, Seki Y, Kurimoto K, Yabuta Y, Yuasa M, Shigeta M, Yamanaka K, Ohinata Y, Saiyou M. 2008. Critical function of Prdm14 for the establishment of the germ cell lineage in mice. Nature Genetics 40:1016-1022.

Yeom Y, Fuhrmann G, Ovitt A, Ohbo B, Gross M, Hibner K, Scholer HR. 1996. Germline regulatory element of Oct-4 specific for the totipotent cycle of embryonal cells. Development 122:881-894.